Bell Canyon Field Trip Guidebook

Facies Architecture of Submarine Channel-Levee and Lobe Sandstones: Permian Bell Canyon Formation, Delaware Mountains, West Texas

Mark Barton

November 21-23, 1997

Sponsored by

DOE ~~PTTC~~ STARR

Bureau of Economic Geology

Noel Tyler, Director

The University of Texas at Austin
Austin, Texas 78713-8924

Cover: Photograph shows crosscutting channels stacked in an offset fashion. Beds within the upper channel extend in a continuous fashion over the channel margin and into adjacent overbank areas. In doing so, the beds thin, decrease in dip, and change facies from cross-laminated sandstones in the channel to thin-bedded rippled laminated sandstones on the flank.

Contents

Figures

Tables

Introduction

The Bureau of Economic Geology at The University of Texas at Austin recently conducted an outcrop characterization study of Bell Canyon exposures as part of a reservoir characterization project funded by the U.S. Department of Energy (DOE). The project focused on slope and basin clastic reservoirs of the Delaware Mountain Group of West Texas and Southeast New Mexico reservoirs because of the significant resources they contain and the complex internal architecture and distribution of petrophysical properties they display. The outcrops were examined to provide unambiguous and high-resolution information on sandstone body and seal architecture. In addition to the outcrop study, the project involved field studies of two Delaware Mountain Group reservoirs (Geraldine Ford and Ford West), a 3-D seismic survey, a petrophysical study of the Ramsey Sandstone within the Geraldine Ford field, and a reservoir simulation within a portion of the Geraldine Ford field.

On this trip, we will visit exposures of the Bell Canyon Formation that were deposited in the deep-water Delaware Basin during the late Permian. The origin of these sandstones has been a source of controversy, with depositional interpretations ranging from contourites, turbidity current deposits, and saline density currents deposits. Our outcrop study focuses on a stratigraphic unit in the Bell Canyon Formation that is analogous to the highly productive Ramsey Sandstone. This unit shows complex stacking patterns and facies changes that are related to the progradation and retrogradation of a system of channel levees and attached lobes. The guidebook provides most of the geological background necessary for this trip as well as data (maps, photographs, logs, and cross sections) and discussions relevant to each field trip stop. Issues to be addressed will include the recognition and correlation of key surfaces, the distribution of facies, and processes responsible for how the sandstones were deposited.

Regional Setting and Stratigraphic Framework

The Bell Canyon Formation is a deep-water siliciclastic unit that accumulated in the Delaware Basin during the Late Permian. The Delaware Basin, located in West Texas and southeast New Mexico, is a circular basin about 120 mi in diameter (Figure 1). The basin was semirestricted with its southern end partially open to the seaway and its northern end surrounded by an extensive carbonate shelf and reef complex. Shelf-to-basin-floor correlations of time-equivalent strata indicate water depths were between 1,000 and 2,000 ft during deposition of the Bell Canyon Formation (Kerans and others, 1992).

The Bell Canyon is the youngest formation in the Delaware Mountain Group, which also includes, in ascending stratigraphic order, the Brushy Canyon and Cherry Canyon Formations (Figure 2). The Bell Canyon Formation is composed of sandstones, siltstones, and minor amounts of carbonate. Clay-sized material is almost completely absent. Maximum thickness of the Bell Canyon Formation is about 1,200 ft near the center of the basin. Near the margins of the basin it interfingers with and onlaps adjacent carbonate slope deposits of the Capitan Formation. Time-equivalent shelf strata include, in ascending stratigraphic order, the Seven Rivers, Yates, and Tansill Formations. The Bell Canyon Formation is overlain by gypsum deposits of the Castile Formation.

Basinal limestones and organic-rich siltstones divide the Delaware Mountain Group at several scales into cyclic successions of sandstone and siltstone (Jacka and others, 1968; Meissner, 1972, Jacka, 1979; Gardner, 1992). At least three scales, classified as low, intermediate, and high, have been recognized (Figure 3). At the largest scale (low order), thick limestones or organic-rich siltstones that are basinwide in extent, divide the Delaware Mountain Group into three clastic wedges. These clastic wedges are 1,000 to 1,500 ft thick and roughly approximated by the Brushy Canyon, Cherry Canyon, and Bell Canyon Formations. At the intermediate scale, limestones and multiple, thin, organic-rich siltstones subdivide each clastic wedge into sandstone bodies that are 100 to 300 ft in thickness. The Bell Canyon Formation contains five limestone tongues that, from oldest to youngest, include the Hegler, Pinery, Rader, McCombs, and Lamar. These limestone tongues extend basinward from the shelf margin and divide Bell Canyon into five sandstone bodies or intermediate cycles that are informally labeled BC-1 through BC-5 in ascending stratigraphic order (see figure 3). The sandstone bodies are further subdivided by thin organic-rich siltstones into units referred to as high-order cycles (Gardner, 1992). The high-order cycles are 20 to 100 ft thick and tend to show a trend of upward-increasing followed by upward-decreasing sandstone content.

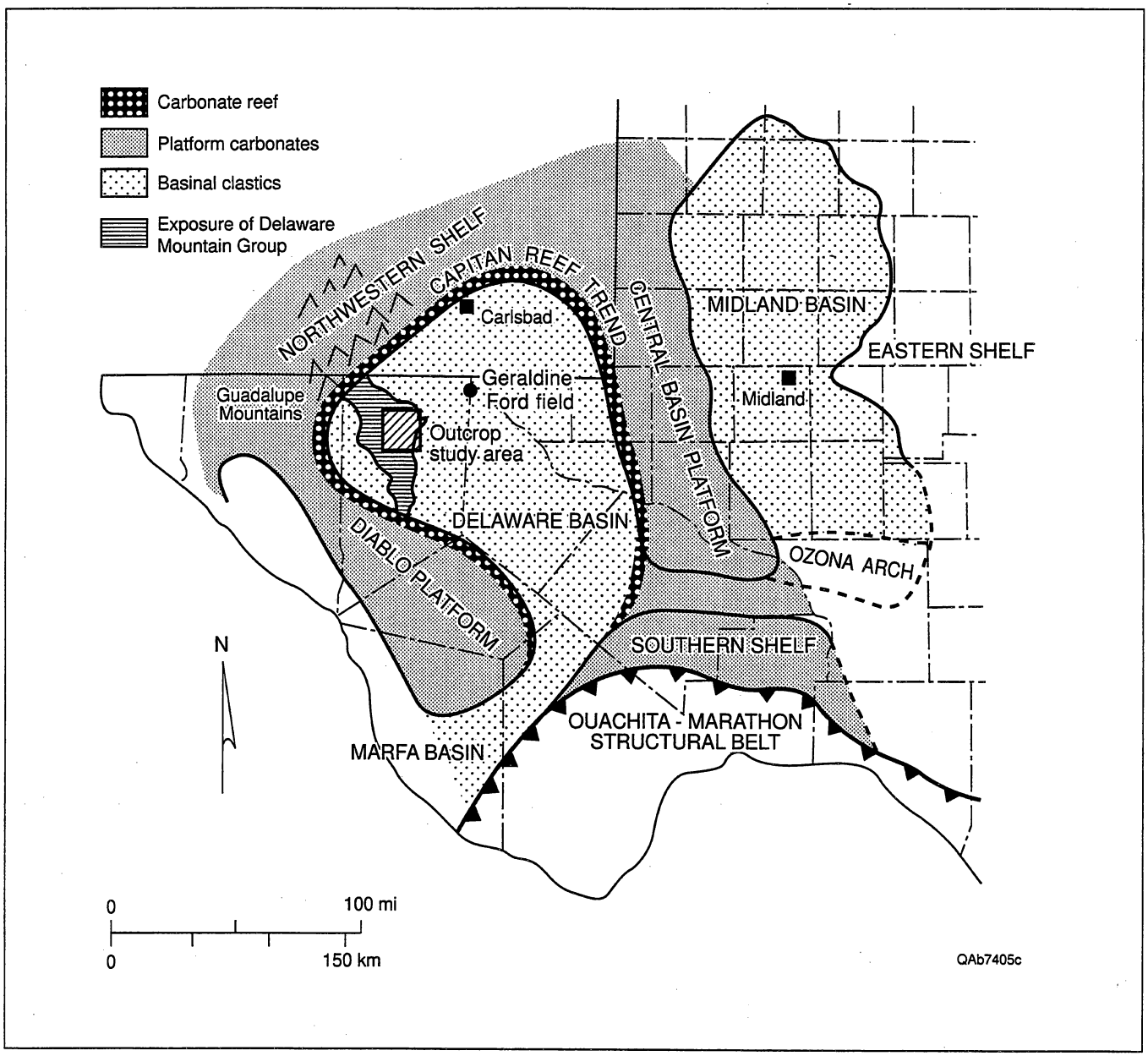

Figure 1. Map showing location of Delaware Basin and paleogeographic setting during the Late Permian.

The cyclic interbedding of sandstones and siltstones with organic-rich siltstones and limestones has been interpreted by some to record frequent changes in relative sea level (Meissner, 1972). During highstands in relative sea level, sands were trapped behind a broad, flooded shelf and prevented from entering the basin. Thin, widespread, organic-rich siltstones accumulated on the basin floor through the slow settling of marine algal material and airborne silt. Basinal limestones were deposited by sediment gravity flows that originated from the slumping of carbonate debris along the flanks of a steep, rapidly aggrading carbonate platform. During subsequent lowstands in relative sea level the carbonate shelf was exposed and sandstones bypassed to the basin floor. Textural characteristics of the sands, such as the absence of clay-sized material, and the lack of channels on the shelf suggest wind was an important agent in transporting the sands to the shelf margin. Paleocurrent indicators suggest the sands entered the basin from the Northwest Shelf and Central Basin Platform.

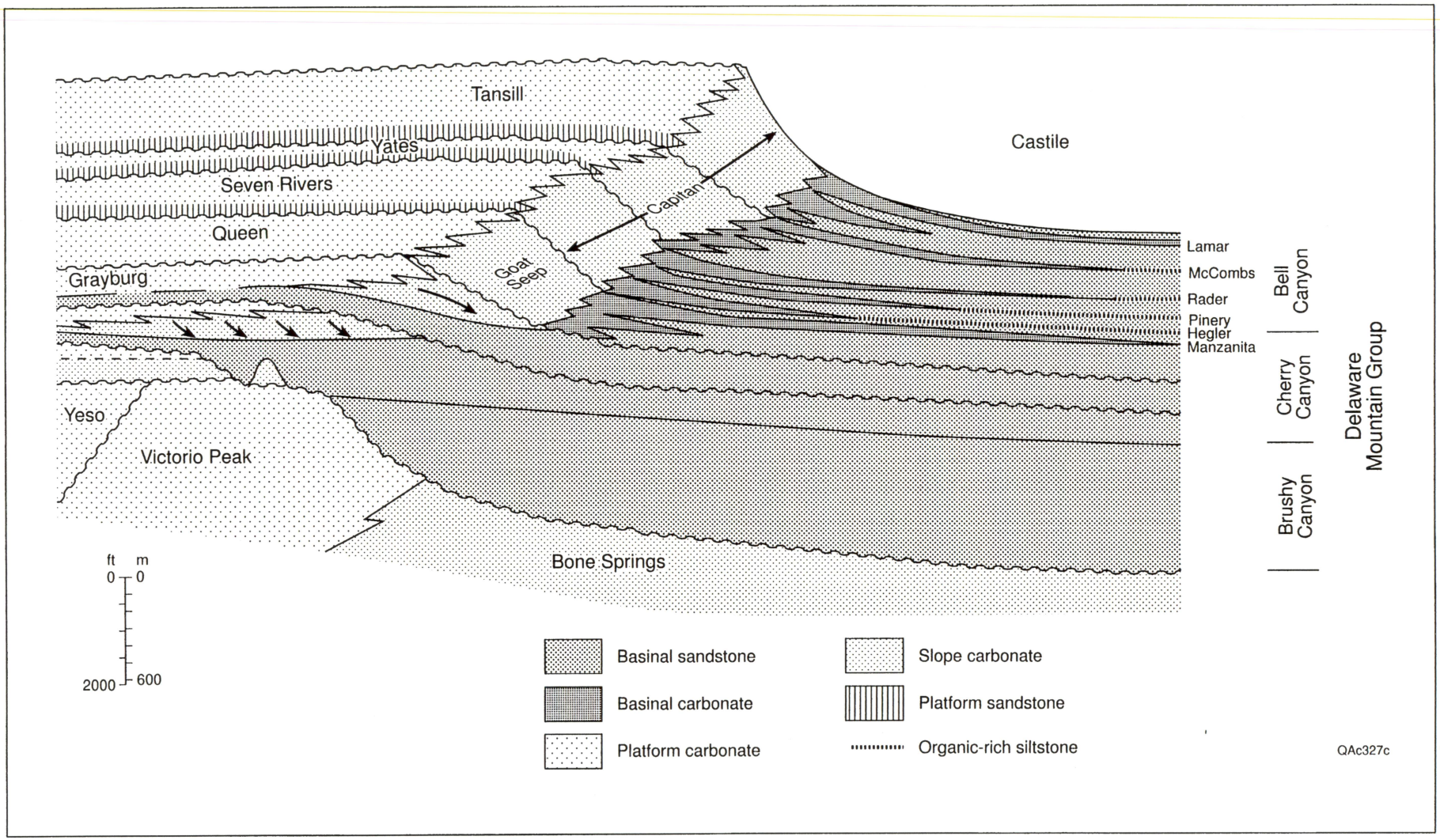

Figure 2. Cross section through northwestern part of the Delaware Basin illustrating Late Permian stratigraphy. Adapted from Kerans and Fitchen (1995) and Sonnefeld (1991).

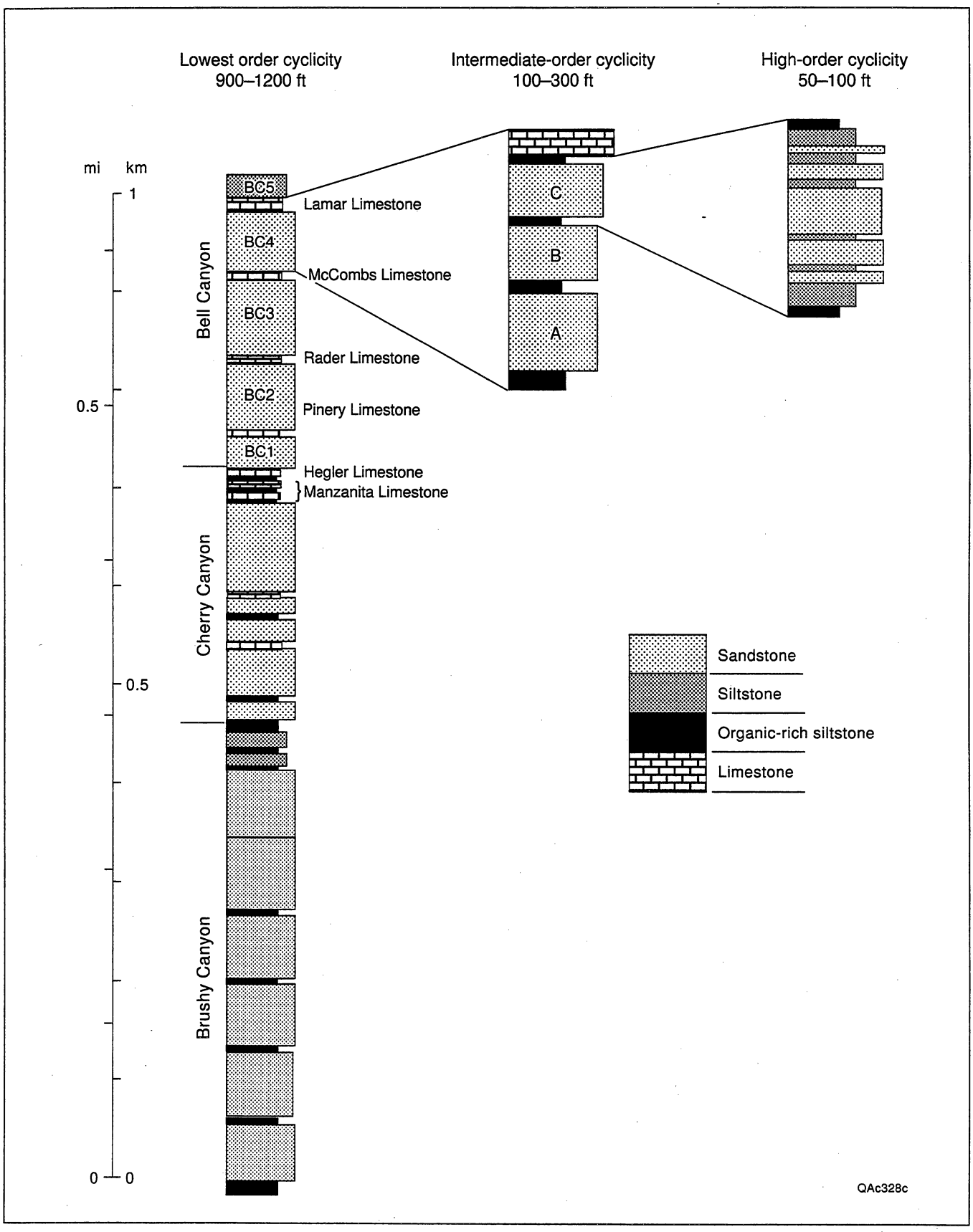

Figure 3. Diagram illustrating stratigraphic cyclicity within Delaware Mountain Group. Three scales classified as low, intermediate, and high have been recognized. Modified from Gardner (1992).

Models of Basinal Sandstone Deposition

It has been shown that production from many Bell Canyon reservoirs comes from the distal end of long, linear sandstones bodies that extend basinward from the shelf margin (Williamson, 1978) (Figure 4). Although this feature has been recognized for some time, the processes that deposited the sandstone bodies have been the source of considerable controversy. Most investigators agree that the sands were carried into the basin by density currents. However, disagreement exists over whether the currents derived their higher densities from a high suspended sediment load (sediment gravity flow) or high salinities (saline density current). The significance of the disagreement has importance with regard to predicting sandstone distribution and reservoir architecture.

In the sediment gravity flow model, dense sediment-rich mixtures were generated on the shelf edge by the slumping of sand masses that had accumulated by eolian processes during lowstands in relative sea level (Fischer and Sarnthein, 1988) (Figure 5). Density differences between the sediment-rich mixtures and ambient waters caused them to moved downslope as turbulent sediment gravity flows (Payne, 1976; Berg, R. R., 1979; Jacka, 1979; Zelt and Rossen, 1995; Bouma 1996). The flows passed through channels and emerged on the basin floor where they spread as unconfined flows. Flows that spilled over the channels deposited sediment to form levees adjacent to the channels. The model predicts that clean channel sands are flanked by wedge-shaped levee deposits composed of interbedded sandstone and siltstone. Basinward, the channels bifurcate and terminate in broad, fan-shaped lobes of sand that are interstratified with siltstone deposited from the fallout of airborne silt or derived from density interflows. The model predicts that systematic changes in facies should be developed as the system progrades and the lobes are overlain and incised by channels and levees (Figure 6). Sandstones displaying traction-produced stratification should be rare, while structureless, graded sandstones displaying partial Bouma sequences should be relatively common.

In the saline density current model, dense saline fluids were generated behind a carbonate reef by evaporation (Harms, 1968, Harms, 1974; Williamson, 1977; Williamson, 1978; Williamson, 1979; Bozanich, 1979; Ruggiero, 1985; Harms and Williamson, 1988) (see figure 5). The dense fluid moved down the slope and into the basin carrying with it entrained sediment. Along the way, currents scoured out channels and deposited sands in those channels during subsequent flows. Less dense flows moved into the basin as density interflows, depositing topography-mantling siltstones from suspension. The model predicts that sandstones should be restricted to infilled scours or channels that lack adjacent levees or distal lobes. The sandstones are interstratified with topography-mantling siltstones that extend into interchannel areas (see figure 6). Sandstones should consist largely of traction-produced stratification, and systematic change in facies should be poorly developed.

Study Area

The Bell Canyon Formation is exposed in the Delaware Mountains of West Texas (Figure 7). The Delaware Mountains extend southeast from the southern end of the Guadalupe Mountains for a distance of about 50 mi. The trend of the Delaware Mountains roughly parallels the direction of sediment transport to the south and southeast in this part of the Delaware Basin (Williamson, 1979). The Guadalupe Mountains define the northwest margin of the basin and expose deposits of an ancient carbonate platform. Bedding surfaces within the carbonate reef and slope deposits dip steeply into the basin, dropping as much as a 1,000 ft over the distance of less than a mile.

The outcrops examined in the study are located on Cowden Ranch, Culberson County, Texas, about 20 mi southeast of the Guadalupe Mountains. Most of the outcrop work focused on stratigraphic relationships within the uppermost high-order cycle in BC-3. The top of this high-order cycle is represented by the McCombs Limestone, and the base by the first regionally correlative organic-rich siltstone. The scale and position of this stratigraphic unit are directly analogous to the highly productive Ramsey interval that correlates with the uppermost high-order cycle in BC-4.

Sedimentology

The outcrops were characterized by mapping facies and bounding surfaces. The data consist of measured logs and photomosiacs that provide complete coverage of the outcrops. Facies is a widely used term for grouping rock types on the basis of origin or any number of similar characteristics. Here, facies are used to define groups with similar sedimentary features at the laminae to bed scale. Bounding surfaces represent breaks in sedimentation that may be erosional or conformable. They record a hierarchy of events that range in scale from individual laminae to basinwide unconformities or flooding surfaces. Bounding surfaces can be classified according to order and type. The

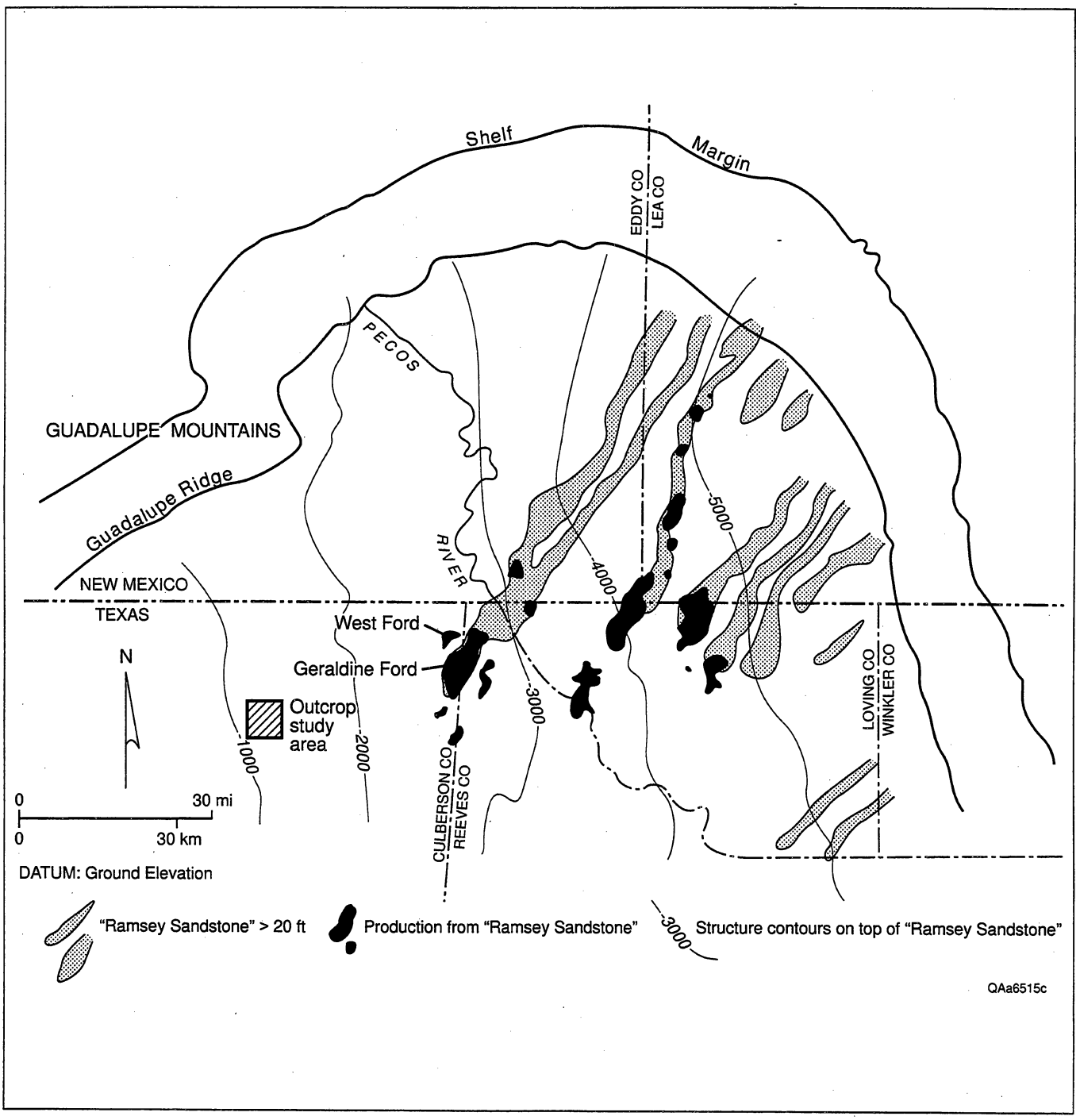

Figure 4. Production from Bell Canyon fields is from the distal (southwest) ends of linear northeast oriented, eastward-dipping sandstone bodies. Map is of the "Ramsey Sandstone" and modified from Ruggiero (1985), after Hiss (1975) and Williamson (1978).

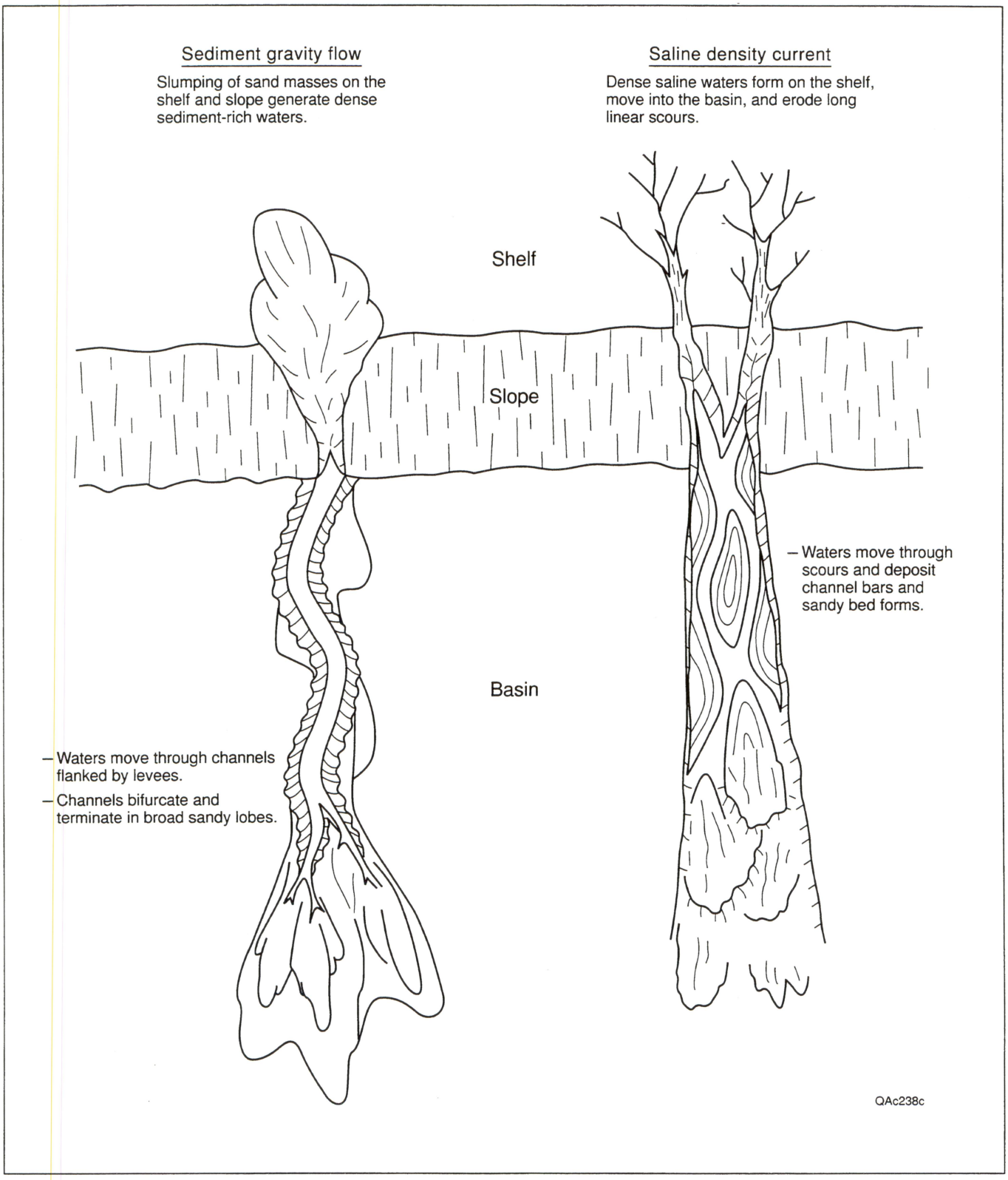

Figure 5. Diagram illustrating the principal depositional models that have been proposed for Delaware Mountain Group sandstones. They include deposition by both turbidity currents and saline density currents.

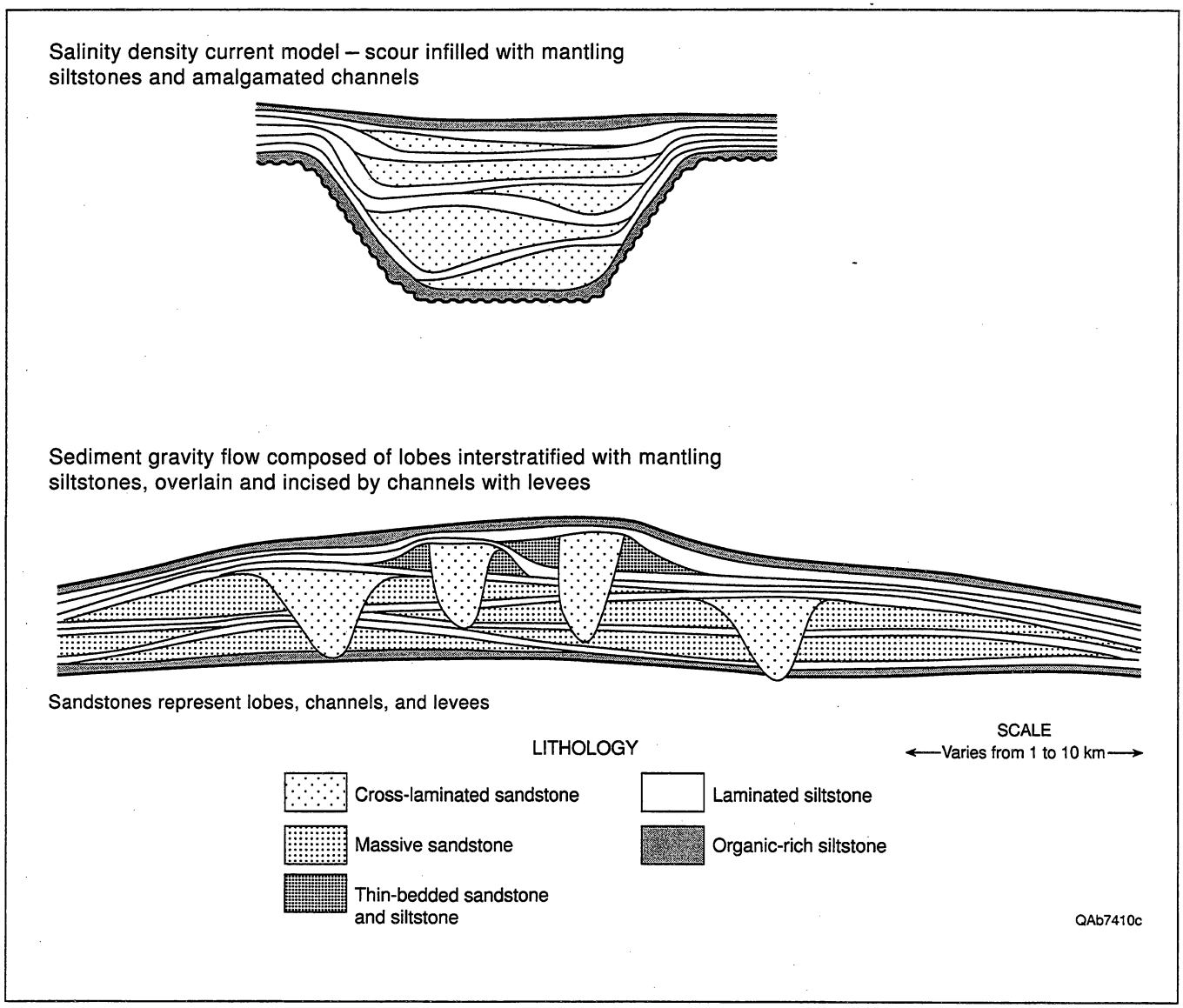

Figure 6. Sand-body architecture for turbidity current model and saline density current model.

mapping of facies together with bedding surfaces has proved to be a useful approach for dividing ancient rocks into sediment bodies that are depositionally related and are characterized by their geometry, lithology, bedding architecture, and scale (Allen, 1983, Friend, 1983, Miall, 1985).

Facies

Six facies are described and categorized by number: facies 1 is an organic-rich, laminated siltstone; facies 2 is a massive organic-rich siltstone; facies 3 is a laminated siltstone; facies 4 is composed of thin-bedded sandstones and siltstones that are graded or display partial Bouma sequences (Bouma, 1962); facies 5 is a structureless sandstone; and facies 6 is a large-scale, cross-laminated sandstone. The six facies are summarized in Table 1 and pictured in Figures 8 through 10. Although most of the sandstones are not graded and do not display classic turbidite-bedding characteristics in the sense of the Bouma sequence, they are interpreted to have been deposited from turbulent sediment gravity flows. This interpretation is based on a variety of features that include bedding architecture, the lack of lamination, and indications of rapid deposition from highly turbulent flows. The absence of lamination or grading may reflect the uniform grain size of the sediment-rich fluids and the

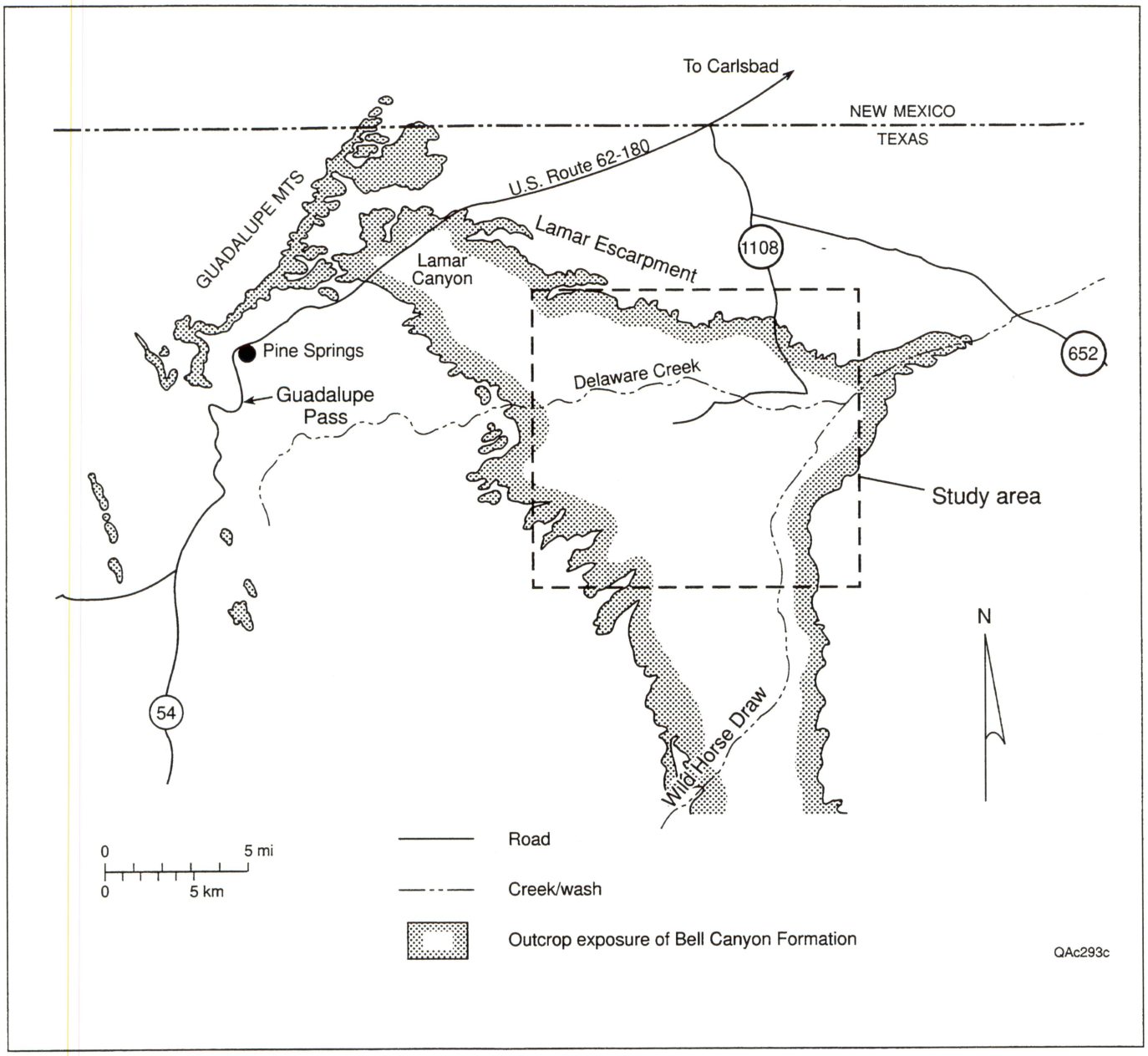

Figure 7. Map showing location of study area and outcrop exposure of Bell Canyon Formation.

rapid fallout of grains from suspension during deposition (Lowe, 1982; Kneller, 1996). The lack of complete Bouma sequences may be due to the fact that the lithologic assemblages that make up a Bouma sequence are areally distributed according to Walther's Law, so that finding true, complete Bouma sequences is difficult (Kneller, 1996).

Facies 1 is a massive, organic-rich siltstone that lacks the extremely fine, parallel lamination of facies 2. It varies in thickness from a few centimeters to a few decimeters and often occurs as a relatively thin, discontinuous drape at the base of a channel or top of a sandstone bed. Contacts with other facies vary from abrupt to gradational with gradational contacts occurring at the top of graded and ripple-laminated sandstone beds. Burrowing is common near the top of the bed. The organic-rich siltstones are interpreted to record the fallout from suspension of silt and organic matter from a turbulent sediment gravity flow. The facies is similar to the E division of the Bouma sequence.

Facies 2 is a dark-gray to black, finely-laminated, organic-rich siltstone. The fine laminations are the result of tan to light-gray siltstone laminae that are a fraction of a millimeter thick. Organic content varies system-

Table 1. Facies characteristics of Bell Canyon sandstone and siltstones.

Facies	Description	Bed Aspect	Transport Mechanisms	Depositional Setting
Facies 1 Massive, organic-rich siltstone	Dark-gray to black. Lacks extremely fine, parallel lamination of facies 1.	Thickness: 0.01 m to 0.3 m Length: 10 m to 1000 m	Suspension deposition from turbidity current. Similar to E division of Bouma sequence.	May occur as discontinuous drapes along the base of channels or along the top of sandstone beds.
Facies 2 Finely laminated, organic-rich siltstone	Dark-gray to black. Often interbedded with centimeters-thick volcanic ash beds.	Thickness: 0.01 m to 1.0 m Length: 10's km	Suspension fallout of pelagic matter and airborne silt.	Deposition during prolonged periods of sediment starvation.
Facies 3 Laminated siltstone	Light-tan to brown. Extremely even parallel lamination that is a fraction of a millimeter to a few millimeters thick.	Thickness: 0.01 m to 3 m Length: Kilometers in length	Regular fluctuations in the settling of marine algal material and airborne silt, or silt derived from low-density interflows.	Occur as laterally extensive sheets that mantle underlying deposits.
Facies 4 Thin-bedded sandstones and siltstones	Current lamination, consisting of ripple drift and to a lesser extent horizontal, are the dominated sedimentary structures.	Thickness: 0.05 m to 1 m Length: 10 to 100 m	Deposition from waning turbidity currents. Similar to BCD division of Bouma sequence.	Deposited along flanks of channel by flows that spill over channel margin.
Facies 5 Structureless sandstone	Sandstones lack lamination and have a massive appearance. Floating silstone clasts, water escape features, and load structures are other common features.	Thickness: 0.1 m to 2 m Length: 100's to 1000's m	Rapid depositon from sediment gravity flow. Equivalent to A division of Bouma sequence.	Deposited at mouths of channels and in overbank areas by unconfined flows. May also occur within upper channel fill.
Facies 6 Cross-laminated sandstone	Dune-scale cross-lamination that varies from infilled scours to climbing dunes.	Thickness: 0.2 m to 20 m Length: 10's to 100's m	Deposition from confined, turbulent, sediment gravity flows.	Largely confined to channels.

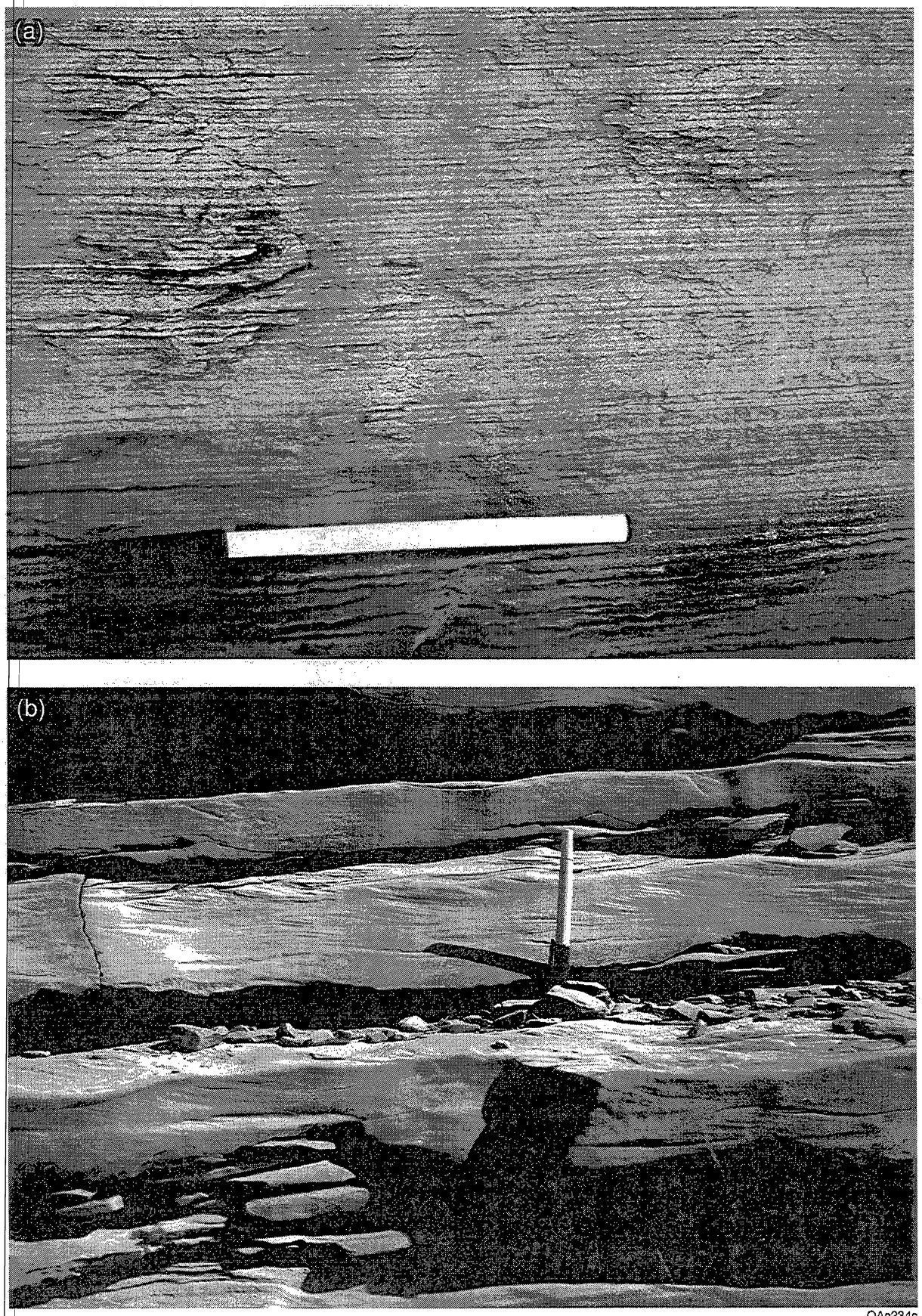

Figure 8. (a) Photographs of laminated siltstone, facies 3. (b) Photograph of facies thin-bedded sandstones and siltstones, facies 4.

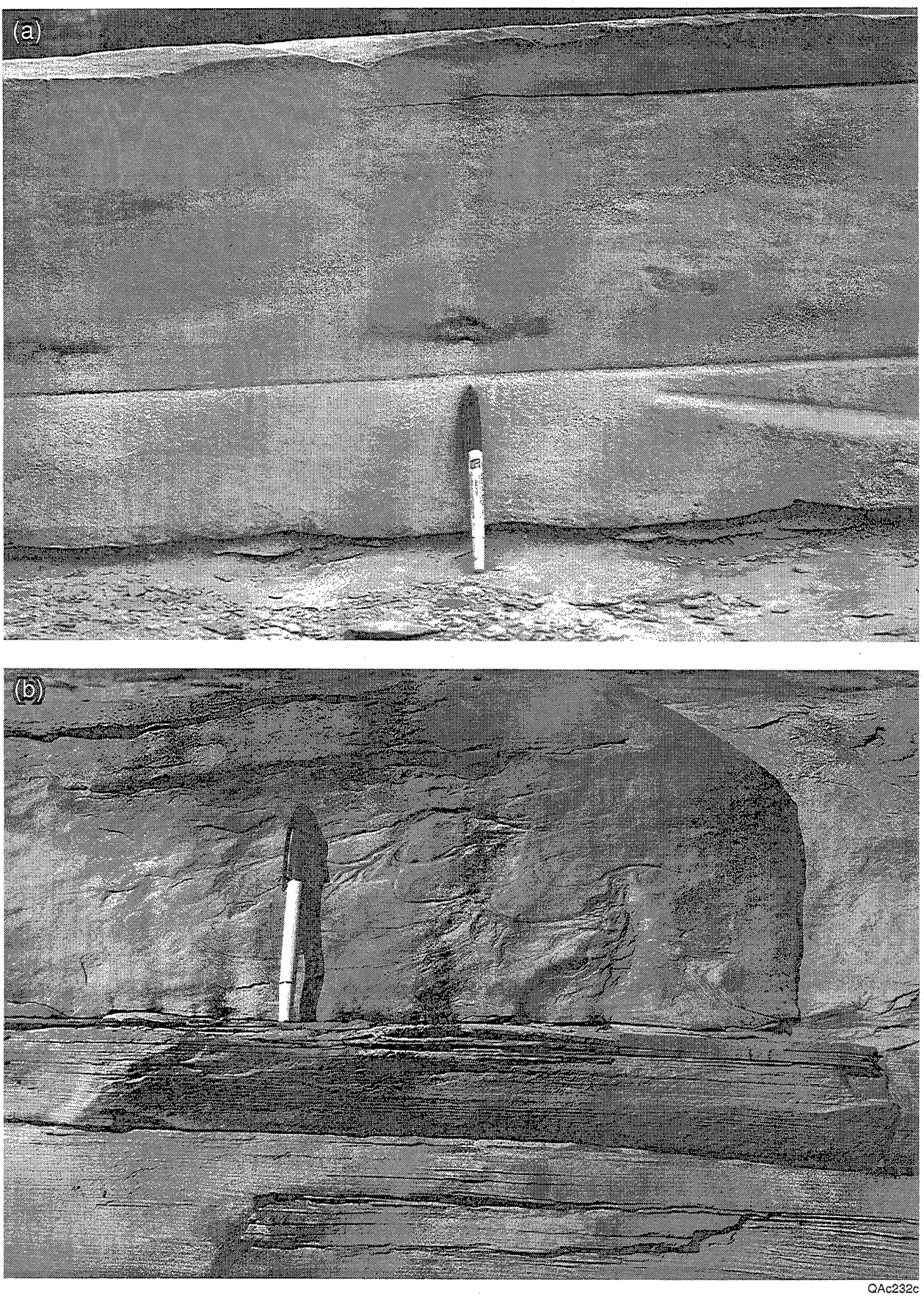

Figure 9. (a) Photograph of structureless sandstone, facies 5. (b) Photograph showing deformed bedding contemporaneous with deposition, facies 5.

Figure 10. (a) Photograph of large-scale cross-lamination, facies 6. (b) Photograph of climbing dunes, facies 6.

atically depending on regular increases or decreases in the thickness of the organic-poor siltstone laminae. Analysis of the organic matter has shown that the majority is derived from marine algal matter (Williamson, 1978; Bozanich, 1979). Fossilized bones or teeth, nodular concretions of chert, siderite, and phosphate, and thin, centimeter-thick beds of volcanic ash are common constituents. Facies 2 displays gradational contacts with facies 3 and occurs at the top of upward-fining, or at the base of the upward-coarsening, successions of laminated siltstone. Facies 2 is interpreted to have been deposited by the settling of marine algal material and airborne silt. The presence of fossils and volcanic ash beds suggests it was deposited during a prolonged period when coarser particles were prevented from entering the basin (Gardner, 1992).

Facies 3 is a laminated siltstone that is similar to facies 2 but contains considerably less organic matter. The dominant sedimentary structure is extremely even, parallel lamination produced by the regular alteration of dark, organic-rich siltstone laminae that are a fraction of a millimeter thick, with tan to light-gray siltstone laminae that are from a fraction of a millimeter to 3 mm thick (Figure 8a). Individual laminae are graded with the transition from light to dark laminae recording a decrease in grain size and an increase in organic matter. Rarely, the siltstone laminae are truncated by shallow scours displaying a few millimeters of relief. The scoured surfaces are usually draped by overlying laminae but may occasionally be overlain by isolated current ripples that are widely spaced, have rounded profiles, and are less than a centimeter thick. Burrowing is not common and is usually restricted to horizontal bedding planes. Laminae are often organized into sets that are a few centimeters to a few decimeters in thickness and show a progressive increase or decrease in laminae thickness or organic content. In turn, the sets may combine to form upward-fining or upward-coarsening successions that are as much as several meters in thickness. The laminated siltstones occur as laterally extensive sheets that mantle underling deposits. Facies 3 is interpreted to record regular fluctuations in the settling of marine algal material and airborne silt or silt derived from low-density interflows. The presence of truncated laminae and current ripples suggests that weak bottom currents occasionally reworked the sediments.

Facies 4 consists of thin-bedded sandstones and siltstones that display an abundance of current lamination (Figure 8b). Sandstone beds are a few centimeters to a few decimeters in thickness and often display erosional bases. Individual beds usually grade upward from sandstone at the base to siltstone at the top. The most common sequence of stratification types is similar to the BC or BCD division of the Bouma sequence with beds beginning with a horizontally laminated sandstone or ripple-drift, cross-laminated sandstone, and passing upward into a wavy-laminated siltstone. Graded sandstones at the base of the bed are rarely observed. The sequence of stratification types and abundance of ripple-drift cross-lamination indicates facies 4 was deposited from waning, turbulent sediment gravity flows.

Facies 5 consists of sandstones that are structureless or massive in appearance (Figure 9a). Sandstone beds are several decimeters to several meters thick and display abrupt, nonerosional bases. Flame structures and convoluted bedding that are contemporaneous with deposition are common at the base of many sandstone beds (Figure 9b). Dewatering features that include dish and pillar structures are common in the upper portions of the beds. Other common features include siltstone clasts that float in a matrix of fine sand and are concentrated near the top of the bed. The lack of lamination, presence of floating clasts, and abundance of water escape and load structures suggest the sandstones were rapidly deposited from high-density sediment gravity flows (Lowe, 1982).

Facies 6 consists of sandstones displaying dune-scale cross-lamination that varies from infilled scours to climbing dunes. The infilled scours are scoop-shaped with sides inclined up to 75 degrees in dip. In plan view the scours have an elliptical shape that is about 4 ft long and 2 ft across. Laminae may onlap the sides of the scour or overlap the margins (Figure 10a). The climbing, dune-scale cross-lamination, often referred to as a mega-ripple drift, is similar to a ripple-drift cross-lamination, only larger in scale. The most common form showed full preservation of laminae on the stoss side of the dune (Figure 10b). Laminae on the lee side of the bed form display tangential bases suggesting the presence of turbulent eddies. The cross-laminated sandstones are restricted to channel fills. The scale, form, and occurrence of the cross-lamination suggests the sands were deposited from confined, highly turbulent sediment gravity flows.

Depositional Elements

Depositional elements are sediment bodies or lithosomes defined by their bounding surfaces, geometry, bedding architecture, and facies. They represent a particular process or suite of processes occurring within a depositional system (Miall, 1985). Depositional elements recognized within the Bell Canyon include: (1) channels; (2) winged channels; (3) lobes; (4) interchannel lobes; (5) sheets of laminated siltstones; and (6) sheets of organic-rich siltstone. The geometry, dimensions, and lithology of the six lithosomes are summarized in Table 2.

Table 2. Characteristics of depositional elements.

Depositional element	Geometry	Dimensions: T-Thickness (m) W-Width (m) AR-Aspect Ratio	Lithology	Depositional Setting/Process
Condensed section	Sheet	T: 0.05 to 0.5 W: 10's km Composite sequences are up to 30 m thick and 100's km in length.	Facies 2 Gradational contacts with facies 3.	Deposition of pelagic material during prolonged period of sediment starvation. Bound stratigraphic cycles at multiple scales.
Siltstone sheet	Sheet	T: 0.1-3 W: Kilometers in length	Facies 3 May form upward-coarsening or -fining successions.	Topography mantling siltstones deposited by density interflows or airborne silt.
Lobe	Broad lens	T: 1-10 W: 1,000-10,000 AR: 100-10,000	Facies 5 Facies 6 near the top of body. Abrupt, nonerosive basal contact.	Sandy lobe deposited by unconfined sediment gravity flows at mouth of channel.
Channel	Convex downward	T: 2-20 W: 10-1,000 AR: 10-100	Facies 6 Facies 5 in upper portion of fill. Facies 1 may drape base of channel.	Incised channel or amalgamated channels.
Winged channel	Biconvex body with wings	Channel: T: 2-20 W: 10-200 AR: 10-20 Wings: T: 1-6 W: 200-2,000 AR: 100-1,000	Channel fill composed of facies 6. Wings composed of facies 4. Facies 1 may drape base of channel.	Aggradational channel levee.
Overbank lobe	Irregular	T: 1-10 W: 1,000 AR: 100-10,000	Facies 5 Facies 6 near top of body. Abrupt, nonerosive basal contact.	Overbank sandstones deposited in topographic lows by unconfined sediment gravity flows.

The channels have a convex-downward geometry. They are bounded at the base by an erosion surface and composed largely of cross-laminated sandstone. The bodies are several meters to 10 m thick and tens of meters to several hundreds of meters in width. Individual channels are often highly truncated and may amalgamate to form a composite body with a larger aspect ratio (50 to 100) than an individual channelform body. The bodies are interpreted as incised channel fills.

The winged-channel elements have a body with a biconvex geometry that is flanked on both sides by beds which gradually thin and taper away from the body. The bodies have an erosive base and are composed largely of cross-laminated sandstones. They vary in size from several meters to several tens of meters in thickness and tens of meters to several hundreds of meters in width. The flanking wings have a wedge-shaped geometry with an aspect ratio of around 100. Thickness varies from 1 to 6 m and length from several hundred to several thousands of meters. The wings consist largely of thin-bedded sandstones and siltstones that tend to become finer grained farther from the channel. Paleocurrents within the wings deviate by about 15 degrees away from the axis of the channel. Bedding features indicate the biconvex bodies are aggradational channel fills and the wings adjacent levees that maintained the channel margins (Mutti and Normark, 1987). The beds are interpreted to have been deposited by turbidity currents that spilled over the margin of the channel.

The broad lens-shaped bodies generally lack an erosive base and are composed chiefly of medium- to thick-bedded massive sandstones. Thicknesses range up to 10 m with aspect ratios on the order of 100 to 10,000. The geometry and abundance of structureless sandstone suggest the lens-shaped bodies were deposited as sandy lobes at the mouth of channels by unconfined, highly depletive sediment gravity flows.

The irregularly shaped sandstone bodies displayed features that are similar to the lens-shaped bodies. They lack an erosive base and consist chiefly of massive sandstones with lesser amounts of cross-laminated sandstones. Width-to-thickness ratios, however, are poorly correlated, and geometry appears to be closely associated with underlying topography. Stratigraphic relationships indicate they are contemporaneous with, or succeed, associated channel-levee deposits. Features of the sandstone and bedding relationships indicate the irregularly shaped bodies were deposited as inter-channel lobes within topographic lows that existed between adjacent channel levees.

The laminated siltstones occur as sheets that mantle underlying deposits. The sheets are less than a meter to more than several meters in thickness. Over an area of 5 to 6 kilometers they displayed little variation in thickness except where they had been incised by overlying channels. The sheets of laminated siltstone were not observed to drape a channel base/margin or occur as part of a channel fill. The uniform thickness and lateral extent suggest the sheets were deposited by airborne silt or laterally extensive, low-density interflows.

The sheets of organic-rich siltstones are similar to the sheets of laminated siltstone but are thinner and less frequent. They occur at the top of an upward-fining succession of laminated siltstone or at the base of an upward-coarsening succession of laminated siltstone. The sheets may combine to form composite sequences that are as much as 30 meters thick and 100s of kilometers in length. The organic-rich siltstone sheets are interpreted as a type of condensed section deposited by the slow settling of marine algal matter during a prolonged period when the basin was starved of sediment. Their distinctive lithology and lateral extent make them excellent correlation markers.

The lithosomes are organized in a systematic fashion to form cyclic successions referred to as high-order cycles. The cycles are bounded by organic-rich siltstones that display gradational contacts with overlying and underlying laminated siltstones. Overlying laminated siltstones at the base of the cycle coarsen upward and are interstratified with broad, lens-shaped sandstone bodies. The succession is locally incised and replaced by amalgamated channels that pass upward into winged channel-form bodies interstratified with irregularly shaped sandstone bodies. The winged channels displayed cross-cutting relationships and stacked vertically and laterally to form multistoried complexes. Channel orientation within a complex varied by as much as 90 degrees. An upward-fining succession of laminated siltstones interstratified with broad, lens-shaped sandstone bodies abruptly overlies the deposits and caps the cycle.

The high-frequency cycle is interpreted to record deposition from a system of channel levees with distal lobes. The multistoried channel complex records repeated episodes of channel aggradation and avulsion. The systematic change in cycle architecture indicates the system prograded into the basin, aggraded, and then retrograded. Bounding, organic-rich siltstones record periods when sediment was prevented from entering the basin.

FIELD STOPS

Day 1

We will depart from Carlsbad, New Mexico, and drive south into Texas. We will visit outcrops of the Bell Canyon Formation that are located on the Cowden Ranch about 10 mi south of the Texas–New Mexico border. We will begin the day by examining limestone and siltstone facies that bound the major sandstone successions (Stops 1.1. and 1.2). We will then focus on the sandstone facies and how they are arranged to form elements that include channels, levees, interchannel deposits, and lobes (Stops 1.3 and 1.4). The location of field trip stops on the Cowden Ranch is shown in Figure 11. A road log to each stop that begins in Carlsbad, New Mexico, is also provided.

Road Log

Mile	
0.0	From Stevens Motel, proceed south on Highway 62/180.
35.1	Turn left and proceed southeast on Highway 652.
40.4	Turn right and proceed south on Road 1108.
42.7	**Stop 1.1.** At speed limit sign, park cars on right side of road.
45.5	At Cowden Ranch proceed west on road 1108.
47.9	**Stop 1.2.** At Delaware Wash, park cars on right side of road.
49.6	At intersection with gas pipeline road, turn left and proceed south on gravel road.
50.1	At crest of saddle, turn right onto dirt road.
51.5	Cross second gas pipeline road and continue south.
53.6	Turn left and proceed east on dirt road.
55.8	Turn left and proceed north on gravel road.
58.1	**Stop 1.3.** At intersection with second gas pipeline road, pull off and park cars on right side of road.
64.7	Retrace route. Turn left at intersection with second gas pipeline road and proceed west.
69.8	At intersection turn left, proceed south, and descend dirt road into Willow Wash.
71.1	**Stop 1.4.** Drive through Willow Wash and park cars on left side of road.

Stop 1.1: Lamar Limestone

Key features

- **Facies of basinal limestone tongue**

The Lamar limestone is the uppermost limestone tongue in the Delaware Mountain Group. It extends across most of the Delaware Basin and separates sandstones and siltstones of intermediate cycles 4 and 5. To the west, near the margins of the basin, the Lamar limestone thickens to more than 100 ft and appears to merge with carbonate slope deposits of the Capitan Formation.

At stop 1.1 the Lamar Limestone is about 2 m thick and is composed of centimeter- to decimeter-thick beds of carbonate mudstone (Figure 12). Individual beds show well-developed grading marked by a color variation from light gray at the base to dark gray at the top. Lenticular chert nodules that are a centimeter or two in thickness and several decimeters long are common in the dark-gray mudstones. The beds have flat, nonerosive bases and show little variation in thickness. Vertically, the beds gradually become thinner by about 50 percent near the top of the succession. Allochems that include fusilinids, crinoids, and brachiopods are not common at this locality, but are abundant at other locations and in other limestone tongues. The Lamar limestone abruptly overlies a laminated, organic-rich siltstone that represents the top of cycle 4. The overlying contact of the Lamar limestone with siltstones of cycle 5 is not exposed at this locality.

The composition and well-developed grading indicate the Lamar limestone was deposited by carbonate-rich turbidites. Stratigraphic relationships, the presence of platform allochems, and the lack of sand or silt, suggest the turbidites were derived from the flanks of a steep, rapidly aggrading, carbonate platform.

Stop 1.2: Delaware Wash

Key Features

- **Facies of basinal, organic-rich siltstones**

The interval is 3 to 4 m thick and composed of six to eight thin (.05 to 0.3 m), organic-rich, laminated siltstones (facies 2) that alternate with (0.1 to 0.5 m)

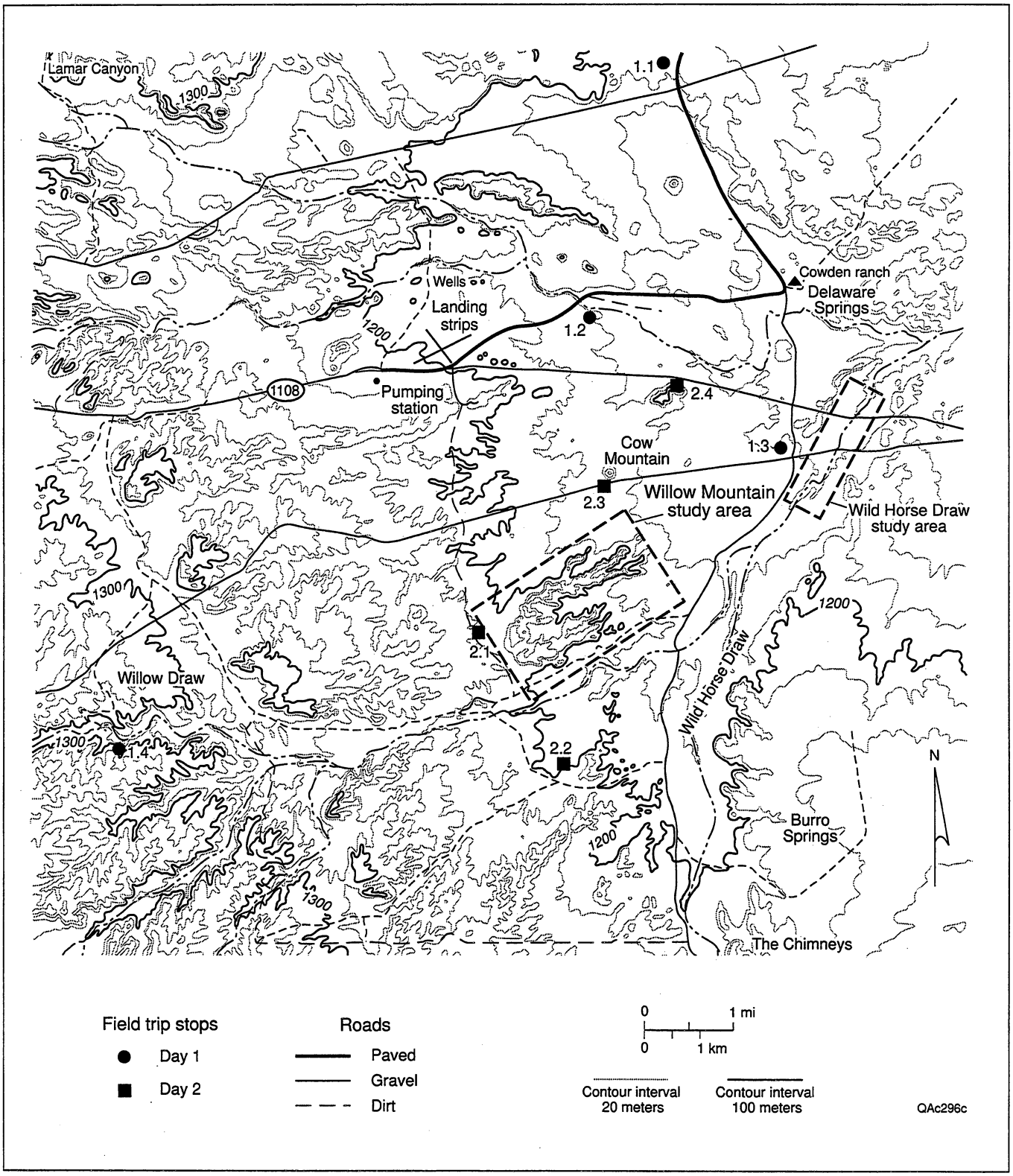

Figure 11. Map showing location of field stops for Days 1 and 2.

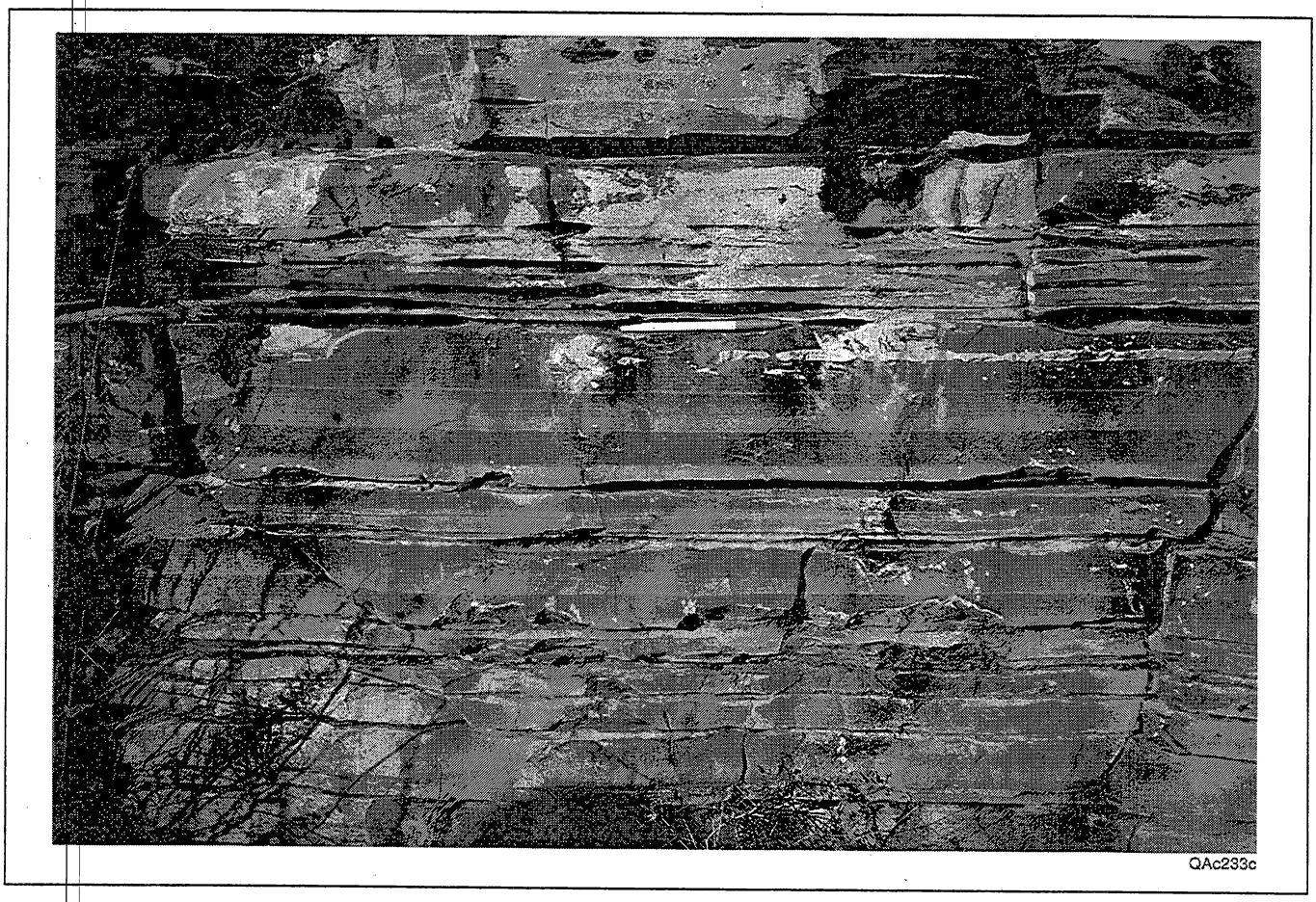

Figure 12. Photograph of graded carbonate mudstones, Lamar Limestone.

laminated siltstones (facies 3). The organic-rich siltstones are dark gray to black and weather dark brown on outcrop. Burrowing is rare to absent throughout most of the interval. Nodular concretions of chert, siderite, and phosphate are common. Thin, centimeter-thick, volcanic ash beds are common within the organic-rich siltstones and tend to weather pink on outcrop. Fossilized bones and teeth have been found in some of the organic-rich siltstones. Lenticular limestone bodies that are 0.1 to 0.5 m thick and several meters to tens of meters in lateral extent are irregularly distributed throughout the interval. The organic-rich siltstones display gradational contacts with underlying and overlying laminated siltstones. Regional correlation has shown that the interval separates sandstones of intermediate-scale cycles 2 and 3. To the west and north the limestones become more continuous and correlate with the Radar Limestone Member of the Bell Canyon Formation.

The abundance of marine algal matter and lack of clay suggests that the organic-rich siltstones accumulated by the settling of marine algal material and airborne silt. The presence of fossilized teeth, bones, and volcanic ash beds suggests rates of deposition were very low and these deposits represent a type of condensed section. Flooding of the carbonate platform during highstands in sea level may have prevented sands from entering the basin and allowed these deposits to accumulate.

Condensed sections combine to form composite successions at several scales. Condensed sections bounding high-order cycles are less than a meter thick and consist of a single, thin, organic-rich siltstone. Condensed sections bounding intermediate-order cycles are 3 to 4 m thick and consist of six to nine organic-rich siltstones. Condensed sections bounding intermediate-order cycles are 20 to 30 m thick consist of 25 to 30 organic-rich siltstones.

The organic-rich intervals form identifiable and correlatable markers both locally and regionally. The condensed sections bounding high-order cycles can be correlated several kilometers or more. They are probably too thin to be resolvable on seismic-scale data sets and may locally be absent due to erosion. The condensed sections bounding intermediate-scale cycles can be correlated at tens of kilometers or more and are thick enough that they may be resolvable on some seismic data sets. The condensed sections bounding low-order cycles can be correlated throughout the basin.

Stop 1.3: Wild Horse Draw

Key Features

- **Sandstone and siltstone facies**
- **Facies and bedding architecture of channel-fill and interchannel deposits**
- **Paleochannel trends and current indicators**
- **Channel geometries and stacking patterns**

Within Wild Horse Draw, the lower part of BC-4 is extremely well exposed. The south end of the wash, although higher topographically, is stratigraphically below the north end. From the southern road that crosses Wild Horse Draw, we will walk to the south end of the wash examining the sandstone and siltstone facies (Figure 13: Stop 2.1a). Then we will turn around and walk back along the exposure and examine how these facies are organized into depositional bodies. Afterward we will walk to the north end of the wash where we will view the pinch-out of several convex-upward sandstone bodies interpreted as lobes (Stop 2.1b).

Stop 1.3a

Along the south end of the wash, a complex of cross-cutting channels and interchannel deposits are exposed within a stratigraphic interval bounded by laminated siltstones (Figure 14). Erosion surfaces divide the channel complex into three bodies. Each body consists of a channel and related interchannel deposit. Erosion surfaces separating the bodies display several meters of relief and are draped in some cases by a relatively thin, massive, organic-rich siltstone. In places, the channels incise completely through the underlying laminated siltstone and organic-rich siltstone. Paleochannel trends, mapped between adjacent walls of the wash, vary by almost 90 degrees (Figure 15). The two oldest channels trend to the southwest, whereas the youngest channel trends to the southeast.

The channels display a biconvex geometry and are 4 to 6 m thick and 30 to 50 m across. The channel fills have a massive appearance and are composed chiefly of large-scale, cross-laminated sandstones. Portions of the fill, especially near the top and center of the channel, may consist of massive or convoluted sandstones often displaying dish structures. Near the base of the channel, sandstones may contain angular to well-rounded siltstone clasts that are up to several centimeters in diameter.

The margins of the channel are draped by a series of beds that have a sigmoidal geometry. The sigmoids are 3 to 4 m in height and dip as much as 20 degrees. Individual beds are as much as a meter thick and tend to thicken toward the axis of the channel. As the beds extend over the margin of the channel, they rapidly flatten and thin by as much as 50 percent. Facies show a change from cross-laminated sandstones within the channel fill to massive and parallel-laminated sandstones over the margin. As the beds flatten and extend into the interchannel areas, facies may show a change to thin-bedded, ripple-laminated sandstones and siltstones. Within the interchannel areas, many of the beds are draped by thin, centimeter-thick massive organic-rich siltstones that pinch out near the channel margins. On both sides of the channel, beds are stacked vertically and slightly offset toward the axis of the channel (Figure 16). As a result, the opposing channel margins are relatively symmetrical with respect to bedding architecture and appear as mirror images.

Within the channels, sandstone beds can be traced into adjacent interchannel areas where they begin to gently dip away from the axis of the channel with some initially slightly thickening. Laterally, however, the beds gradually thin and pinch out by downlapping onto an erosional surface that displays several meters of relief. The surface is overlain by a massive organic-rich siltstone that is up to 10 cm thick. Many of the bedsets are also separated by massive, organic-rich siltstones that are several centimeters thick. Beds flanking the youngest channel are composed largely of massive sandstones that, despite thinning and pinch-out, show little lateral variation in the facies. Flame structures are common along the base of many of the massive sandstones and are tilted away from the channel axis. By contrast, the beds flanking the two older channels are composed largely of thin-bedded sandstones and siltstones that show extremely complex and irregular bedding geometries. They tend as a whole to become finer grained and more thinly bedded away from the axis of their respective channels.

The bedding architecture and biconvex geometry suggest the channels vertically aggraded during deposition with little or no lateral migration. The bedding relationships also indicate that the margins of the channels were maintained by levee deposits. The

Figure 13. Map showing location of field stops for Wild Horse Draw.

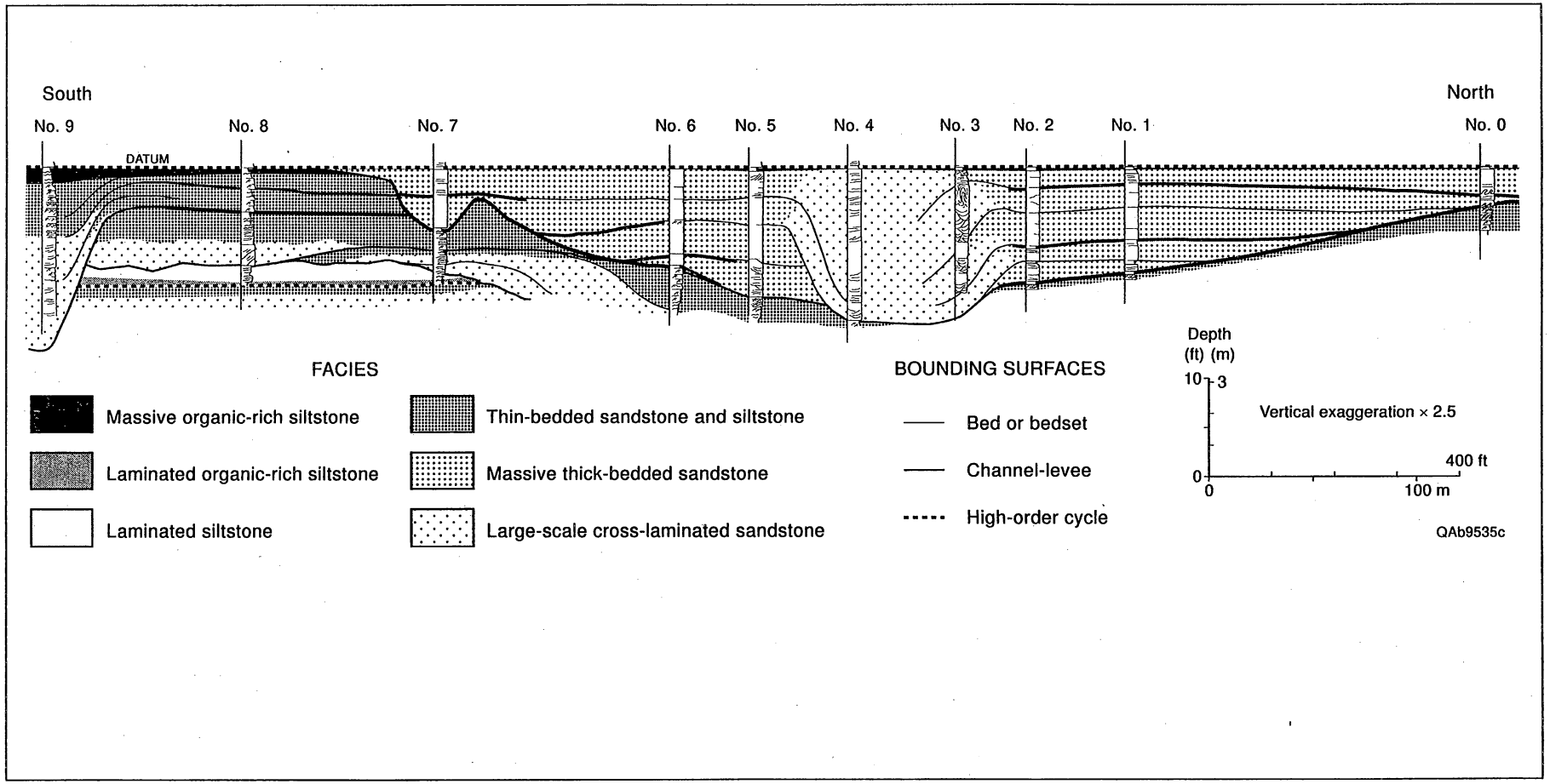

Figure 14. Diagram illustrating facies and bedding architecture from Wild Horse Draw. Exposure is from the north end of the wash along the west wall.

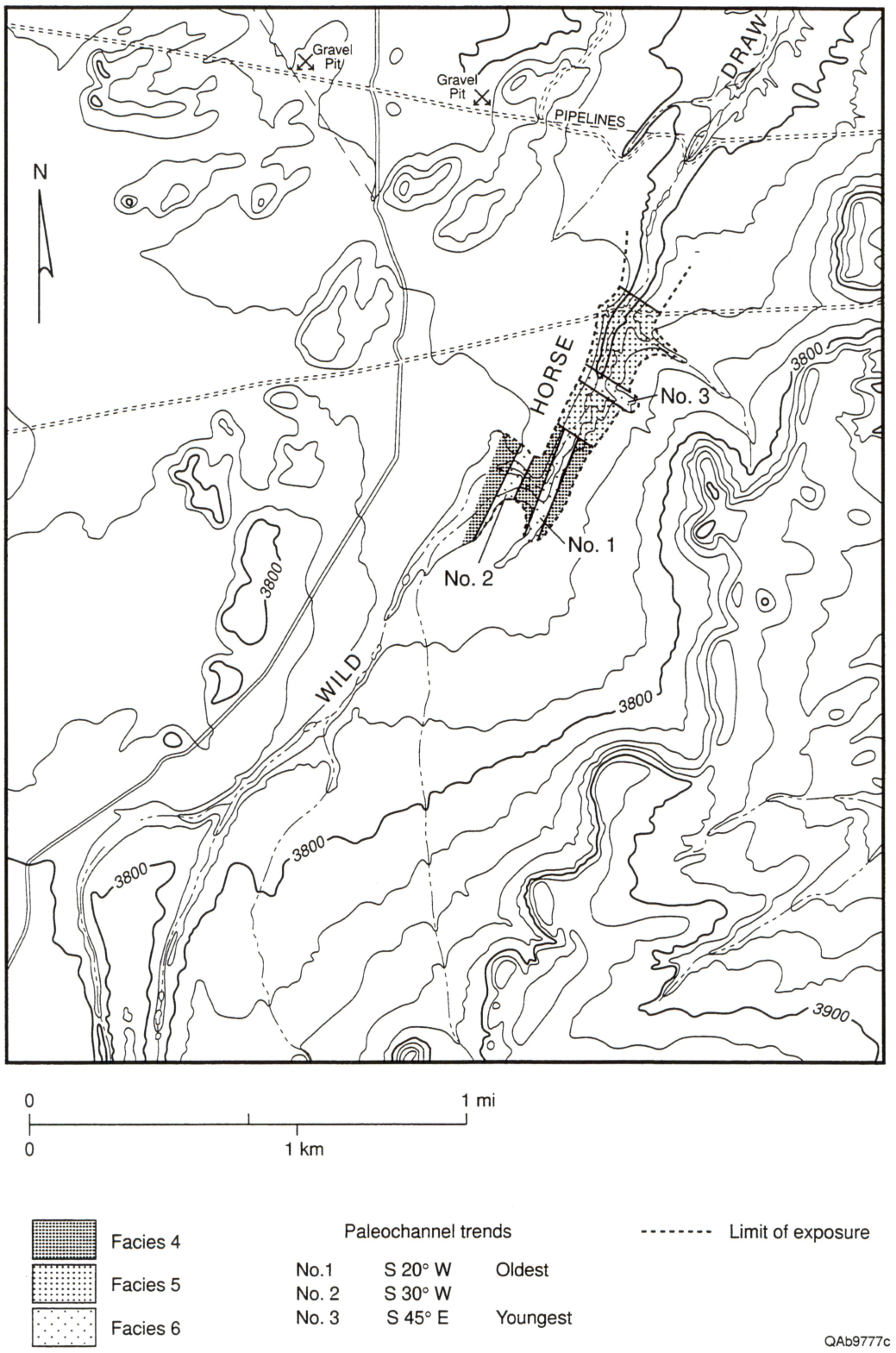

Figure 15. Plan view map showing paleochannel trends from Wild Horse Draw.

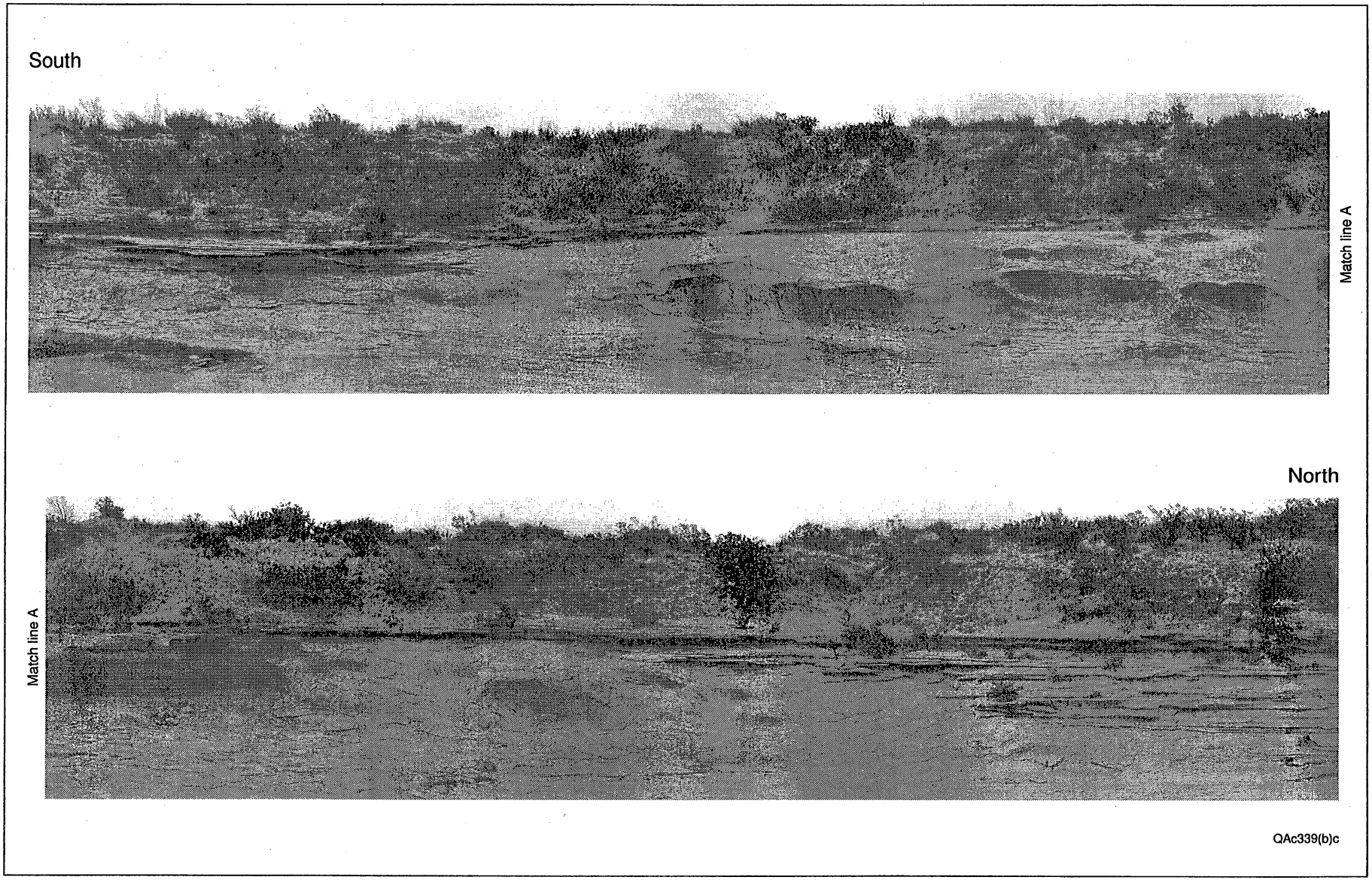

Figure 16. Photograph of channel, Wild Horse Draw.

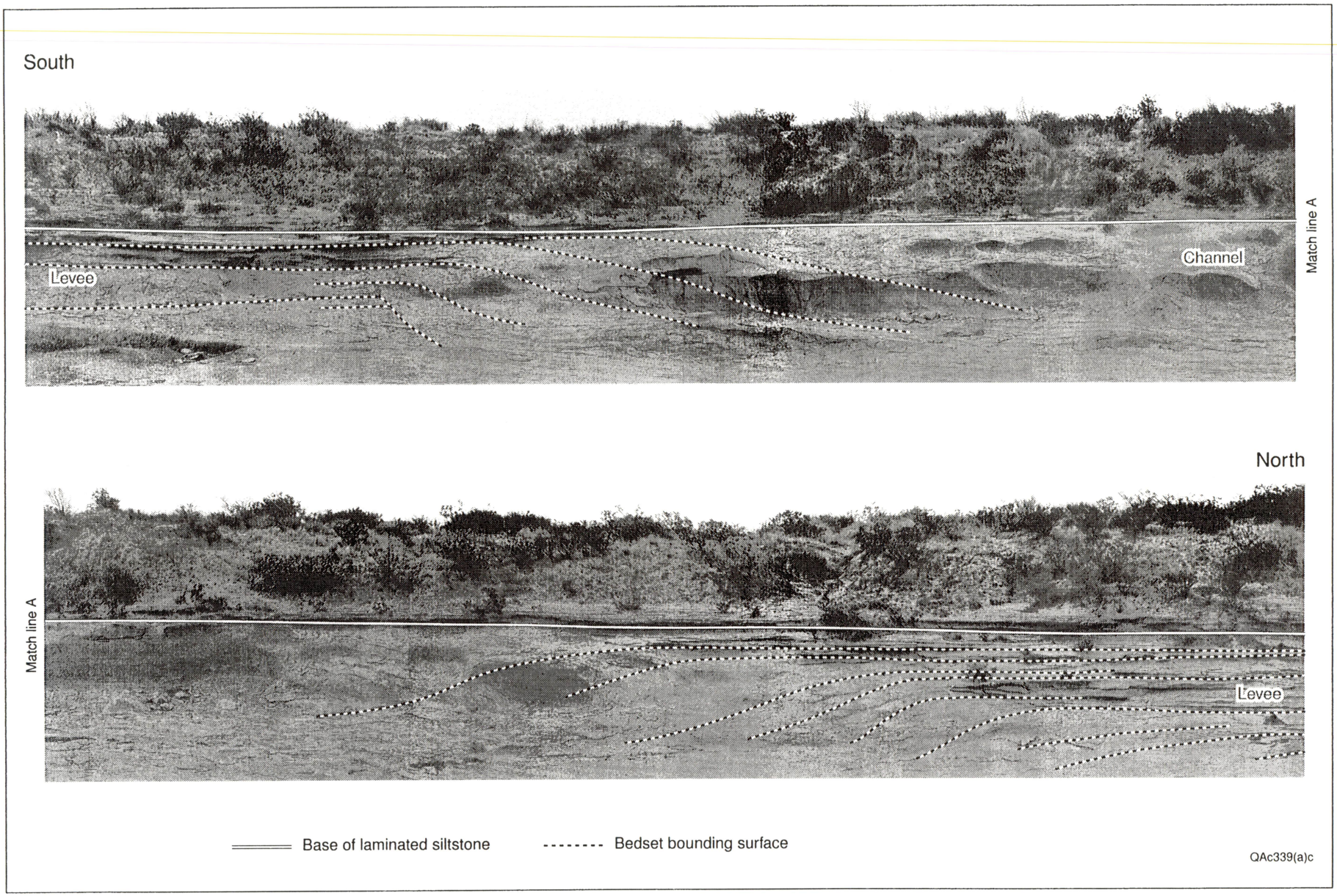

Figure 16. (cont.)

levees are composed of massive sandstones and thinly bedded sandstones and siltstones; cross-laminated sandstones are restricted to the channel fills. The channel stacking pattern suggests that the channels aggraded to the point that they could no longer be maintained by adjacent levees and avulsed into topographically low interchannel areas. It is also important to point out that during each avulsion event, interchannel areas underwent significant erosion. The erosion surfaces are overlain by massive, organic-rich siltstones, current laminated sandstones, and, rarely, a sandstone containing siltstone ripup clasts. The channel architecture and stacking pattern from Wild Horse Draw are interpreted to record a repetition of events that include: (1) erosion; (2) channel aggradation and levee development; (3) channel filling; and (4) channel avulsion (Figure 17).

Stop 1.3b

Along the east wall at the north end of Wild Horse Draw, an interbedded succession of sandstones and siltstones is exposed. The siltstones are laminated and organized into sheets that are 1 to 3 m thick. They are interstratified with broad, lenticular sandstone bodies that are 1 to 2 m thick and largely composed of structureless sandstone. Contacts between the two facies are abrupt but nonerosional. In some places, the sandstone bodies are overlain by massive organic-rich siltstones that vary in thickness from a few centimeters to a few decimeters. As the sandstones are traced to the south, two gradually thin and pinch out over the distance of about 500 m. Along the transition, underlying and overlying laminated siltstones maintain a constant thickness.

The uniform thickness of the laminated siltstones suggests that the lenticular sandstone bodies are not broad, shallow channels. The nonerosive base and the lack of lamination indicate the sandstones were rapidly deposited by waning sediment gravity flows most likely in an unconfined setting such as a depositional lobe.

Stop 1.4: Willow Draw

Key Features

- **Facies and bedding architecture of channel fill in Cherry Canyon Formation**
- **Manzanita Limestone**

A portion of a channel fill is exposed next to the road on the south side of the wash (Figure 18). The erosive base of the channel is marked by a concentration of siltstone clasts and isolated sets of cross-laminated sandstone. The initial channel-filling beds run up the sides of the channel and overextend the margin. The beds display a sigmoidal geometry and thicken toward the channel fill. Several of the beds are draped by a thin, massive, organic-rich siltstone. The sandstone beds are weakly graded and are massively- to weakly-laminated. Succeeding sandstone beds tend to thicken, run up the sides of the channel, but pinch out before overextending the margin. The final set of beds onlap the sides of the channel in a relatively horizontal manner. The relatively flat sandstone beds consist mostly of cross-laminated sandstones in the lower part of the channel fill and massive sandstones in the upper part. Current ripples are present at the top of several of the sandstone beds.

In the walls above the wash, the Manzanita and Hegler Limestones are exposed. The succession is about 30 m thick and composed of decimeter- to meter-thick beds of limestones that alternate in a regular fashion with decimeter-thick beds of organic-rich siltstone. The Manzanita and Hegler Limestones mark the contact between the Cherry Canyon and Bell Canyon Formations. It is interpreted to represent a major condensed section separating two low-order cycles.

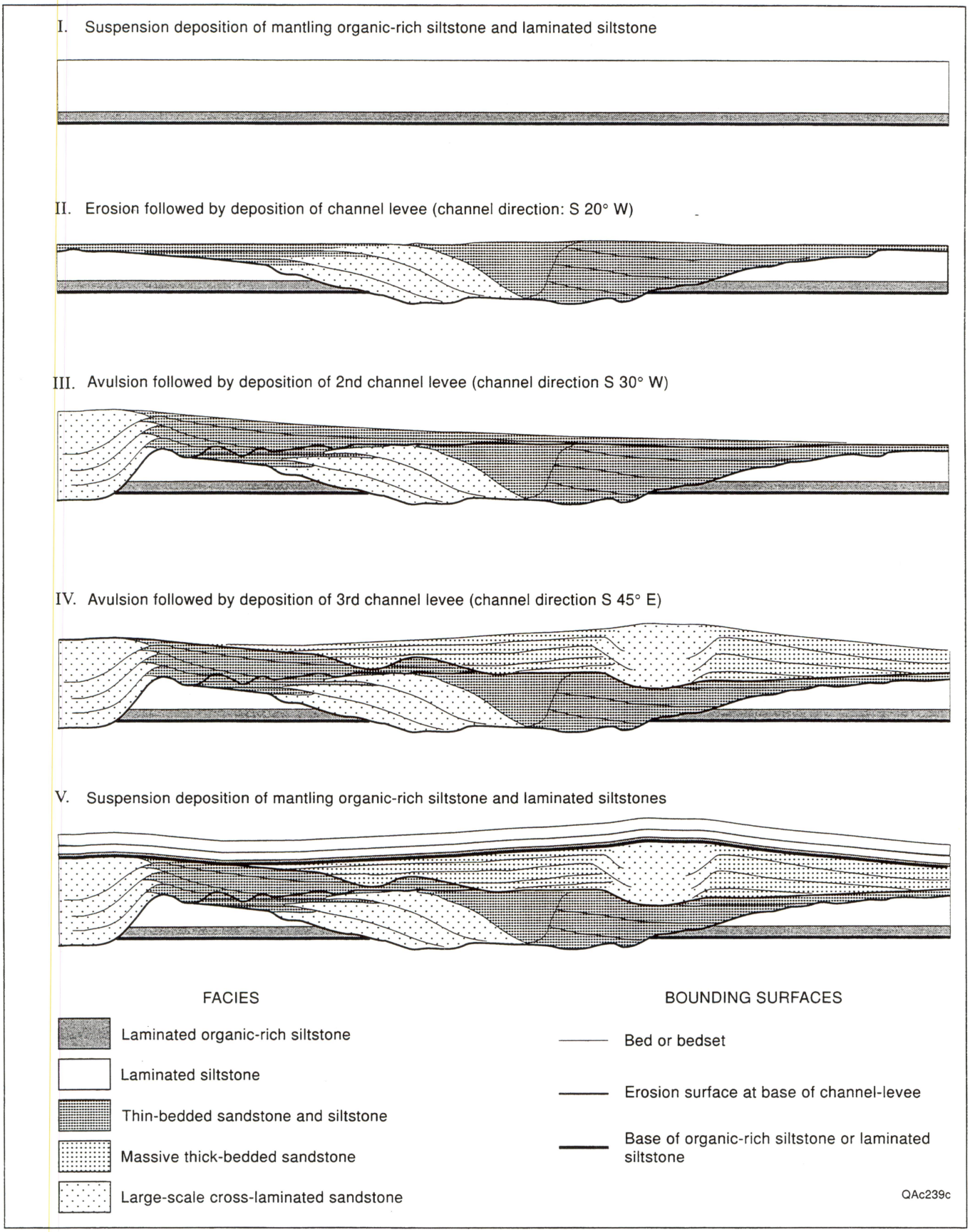

Figure 17. Diagram illustrating the interpreted sequence of events for Wild Horse Draw.

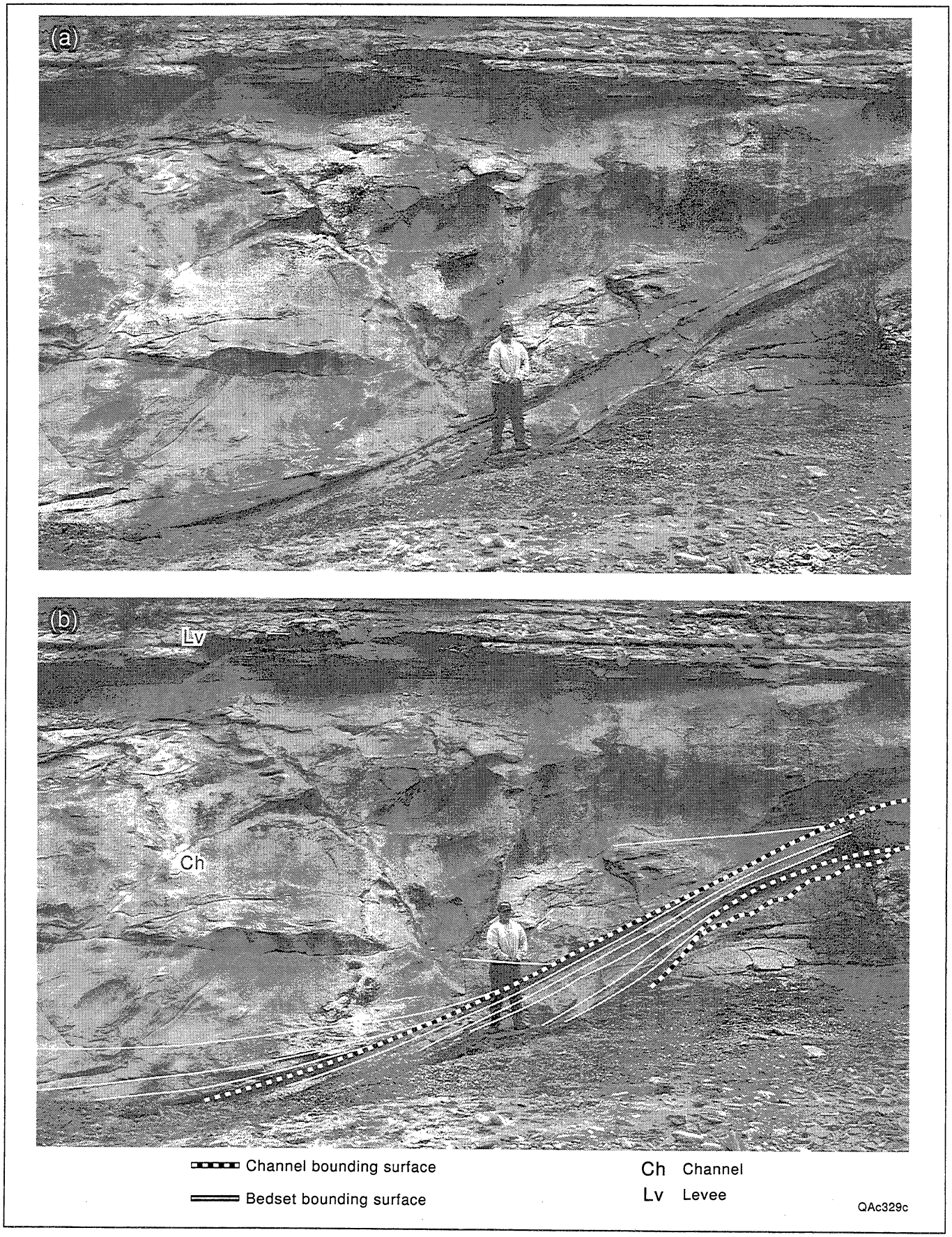

Figure 18. Photograph of channel from Willow Draw.

Day 2

On day 2 we will focus on the arrangement of channels, levees, and lobes within a single high-order cycle. The high-order cycle is bounded by organic-rich siltstones and is positioned near the top of the intermediate cycle BC-3. The scale and position of this stratigraphic unit are directly analogous to the Ramsey Sandstone.

Road Log

Mile	
0.0	From Stevens Motel, proceed south on Highway 62/180.
35.1	Turn left and proceed southeast on Highway 652.
40.4	Turn right and proceed south on Road 1108.
45.5	At Cowden Ranch, proceed west on road 1108.
49.6	At intersection with gas pipeline road, turn left and proceed south on dirt road.
50.1	At crest of saddle, turn right onto dirt road.
51.5	Cross second gas pipeline road and continue south.
53.2	At crest of hill, park cars on east side of road.
54.0	**Stop 2.1** Retrace route 0.8 mi and park cars on east side of road.
55.1	Proceed south and turn right at intersection.
55.5	Proceed west and turn left at Y in road.
55.6	Cross gate and proceed SW.
55.7	Turn left at intersection and proceed SE.
56.9	**Stop 2.2**
59.8	Retrace route to EW road that passes between Cow and Willow Mountains and turn right.
61.4	**Stop 2.3** Cow Mountain.
65.0	Retrace route to EW gas pipeline road and turn right.
67.4	**Stop 2.4** North Cow Mountain.
69.9	Retrace route to Road 1108 and turn right.
72.0	**Stop 2.5** Park cars and visit buttes north of Delaware Wash.

Stop 2.1: Willow Mountain

Key Features

- **Offset channels**
- **Bifurcating channel system**
- **Sandy overbank lobes**

At Willow Mountain the stacking pattern of channels and lobes was documented over an area of several square miles. A map of the study area and location of lithologic logs are shown in Figure 19. Stratigraphic relationships from the north half of the mountain are illustrated in three cross sections (Figures 20-22) labeled A-A′, B-B′, and C-C′. The cross sections are 0.5 to 1.5 mi in length and aligned parallel to the depositional strike of the system.

The high-order cycle is 45 to 75 ft in thickness and is bounded by thin, 1- to 2-ft-thick, organic-rich siltstones. The bounding, organic-rich siltstones display transitional contacts with facies 3 and are traceable across the entire study area except where the basal siltstone has been eroded. The cycle thickness correlated with the sandstone content, which varied from 15 to 75 percent. The cycle is composed of two to five distinct sandstones that varied in thickness from 1 to 60 ft. Within the cycle, sandstone thickness varied systematically showing either a trend of upward bed thickening followed by bed thinning or an upward bed-thinning trend that begins with a relatively thick sandstone.

Sandstones in the upper and lower half of the cycle display a broad tabular geometry up to several meters thick and thin to the east (Figure 23). The sandstones are interstratified with sheets of laminated siltstone that are between 3 and 8 ft thick and show little variation laterally in composition or in thickness. Contacts between the tabular sandstones and siltstone sheets are abrupt but nonerosional. The middle of the cycle consists of a heterogeneous mix of lenticular, channel-form bodies interstratified with wedges of thin-bedded sandstone and siltstone and broad, lenticular sandstone bodies. The channel-form bodies are up to 20 m thick and several hundred meters wide and can be traced to the south and southeast for several kilometers. Within the complex, channel-stacking patterns change in a systematic fashion. In the lower part, the channel-form bodies are highly amalgamated and truncated. In the middle part, they are vertically stacked in an offset pattern (Figure 24) and are flanked by wedges of thin-bedded sandstone and siltstone similar to Wild Horse Draw (Figure 25). In the upper part, they bifurcate and are flanked by broadly lenticular sandstone bodies.

Facies relationships and bedding architecture suggests that the high-order cycle was deposited by a system of channel levees with attached lobes that initially prograded basinward, aggraded, then turned around and stepped back toward the shelf (Figure 26). The upward-bed-thickening succession of sandstones and siltstones incised by amalgamated channels (not shown) was deposited during the progradational phase (step II). The vertical stack of channel-levees was deposited during the aggradational phase (step III). The system of bifurcating channels flanked by interchannel

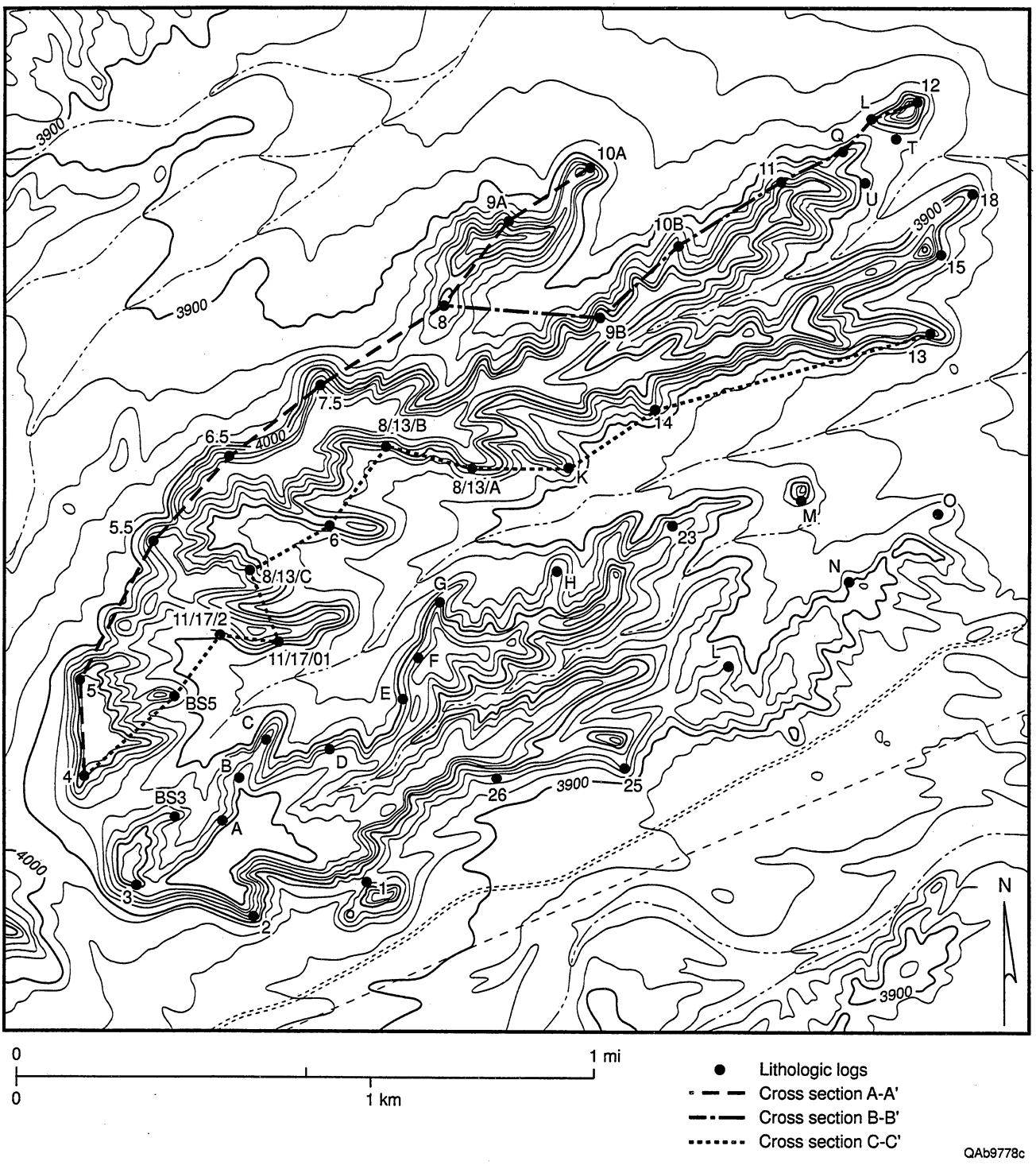

Figure 19. Map of Willow Mountain study area showing location of measured logs and cross sections.

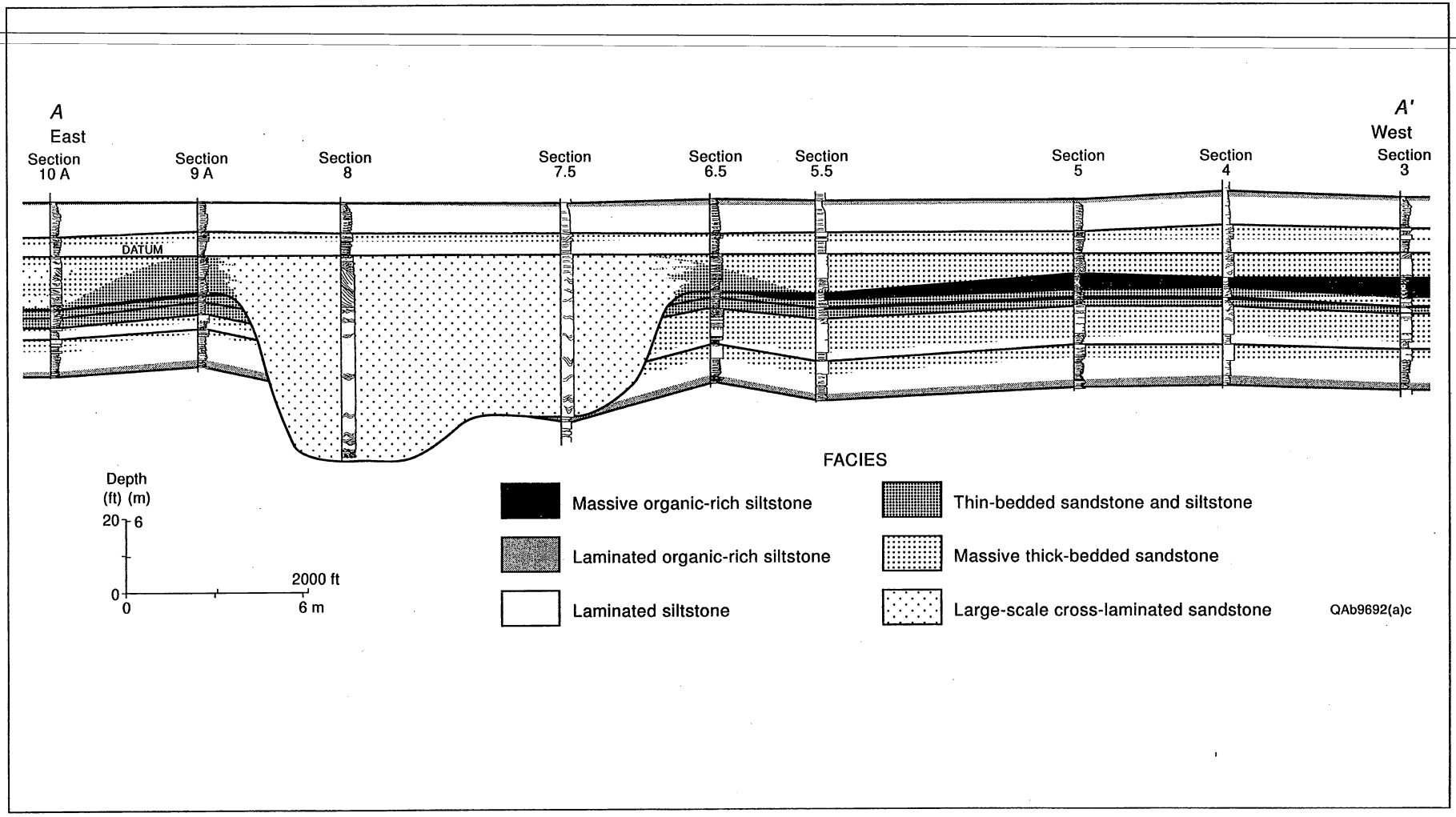

Figure 20. Cross section A–A′ (see Fig. 19 for location) showing distribution of facies and traces of key surfaces within a single high-order cycle, Bell Canyon Formation.

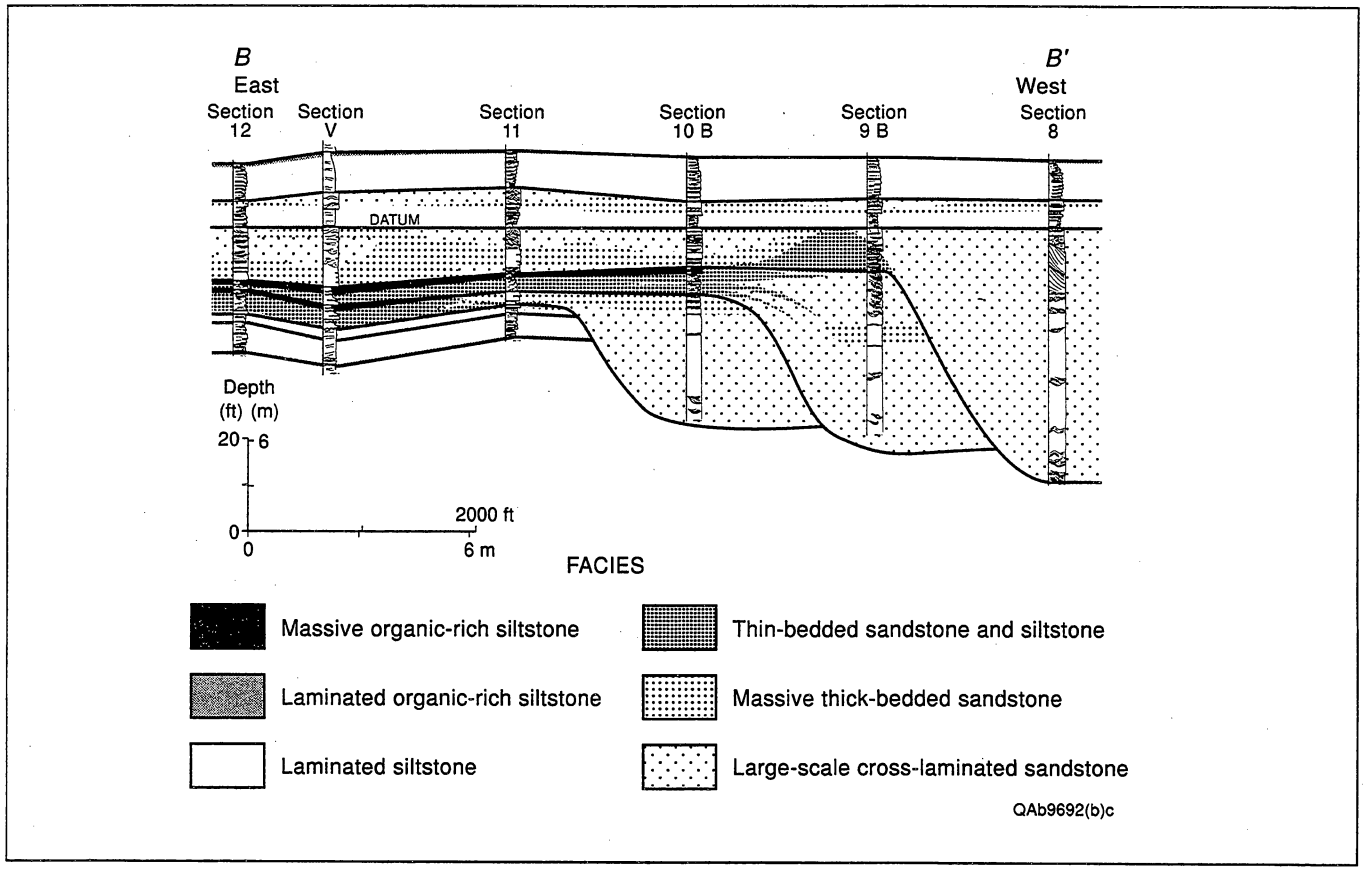

Figure 21. Cross section B–B' (see Fig. 19 for location) showing distribution of facies and traces of key surfaces within a single high-order cycle, Bell Canyon Formation.

lobes was deposited during the retrogradational phase of the cycle. During the retrogradational phase a system of back-stepping lobes may also have been deposited (not shown).

Stops 2.2 - 2.5: South Cowden Ranch; Cow Mountain; North Cow Mountain; Buttes north of Delaware Wash

Key Features

- **Arrangement of channel-levee and lob complexes**

A more regional view of facies and stratal relationships within the high-order cycle seen at Willow Mountain is illustrated in the cross section shown in Figure 27. The cross section extends south from Delaware Wash for a distance of about 6 mi, oblique to the depositional axis of the system. In the cross section, the channel-levee complex exposed at Willow Mountain appears to pass out of the plane of the cross section. Finer grained levees that flanked the margins of the channel form wedges that gradually thin and pinch out over the distance of about a mile (see sections at Cow Mountain, North Cow Mountain, and Stop 2.2).

Further to the south (basinward), near the southern end of Cowden Ranch, the high-order cycle progressively thins to a thickness of about 35 ft and consists of a single sandstone that is about 20 ft thick and bounded by laminated siltstones. The sandstone body has a broad tabular geometry and an abrupt but nonerosive base and is composed largely of structureless sandstones. Organic-rich siltstones above the sandstone body indicate it correlates with the overbank sandstones/lobes at Willow Mountain.

To the north (shelfward), near Delaware Wash, the high-order cycle gradually thickens to more then 80 ft. The increase in thickness is related to an increase in the thickness of sandstones that underlie and overlie the channel-levee and lobe complex exposed at Willow Mountain. Underlying and overlying sandstones cor-

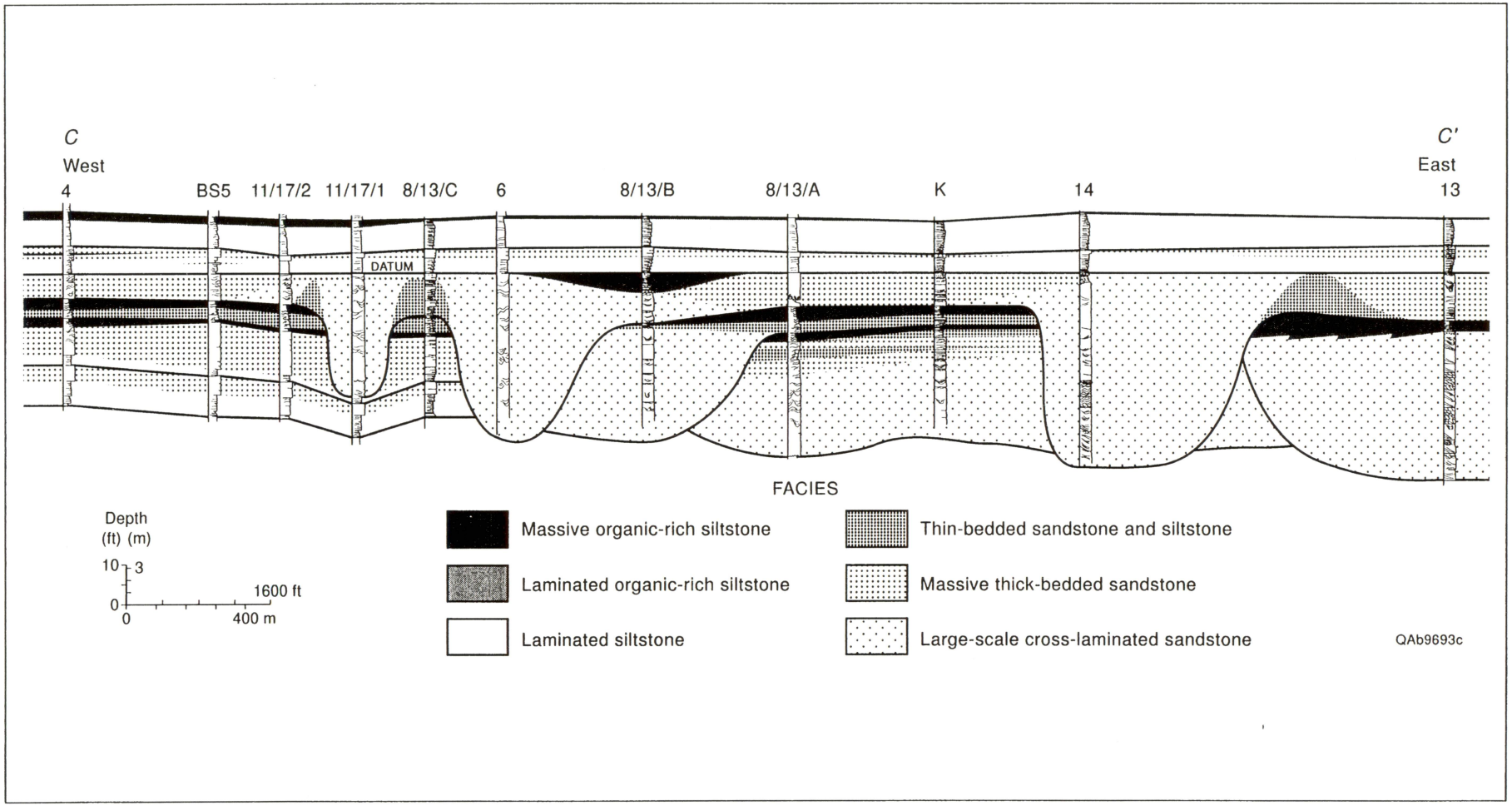

Figure 22. Cross section C–C′ (see Fig. 19 for location) showing distribution of facies and traces of key surfaces within a single high-order cycle, Bell Canyon Formation.

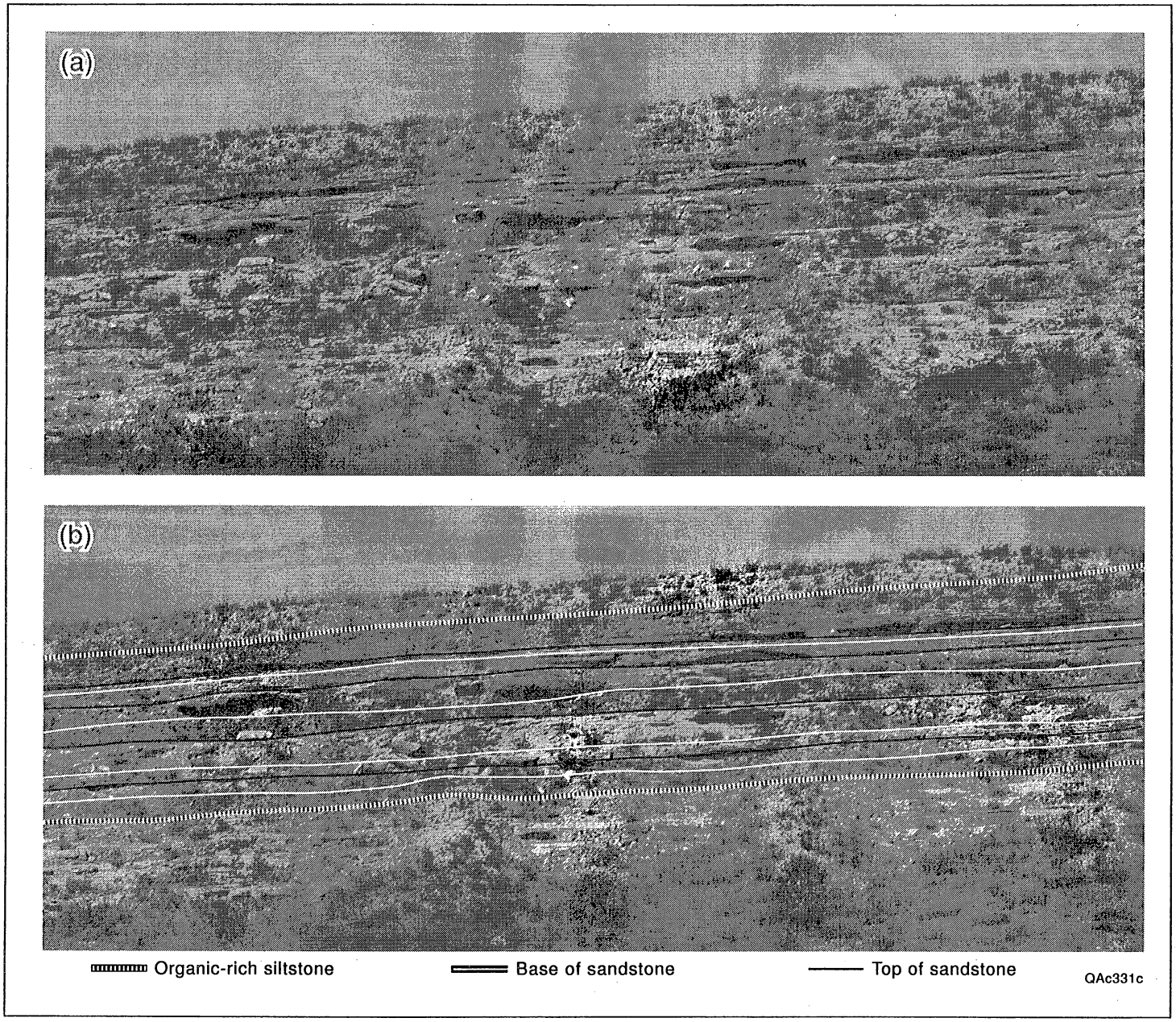

Figure 23. Photograph illustrating sandstone architecture of high-order cycle. Photograph is from Willow Mountain between lithologic logs 4 and 5 (see Fig. 19 and cross section A–A').

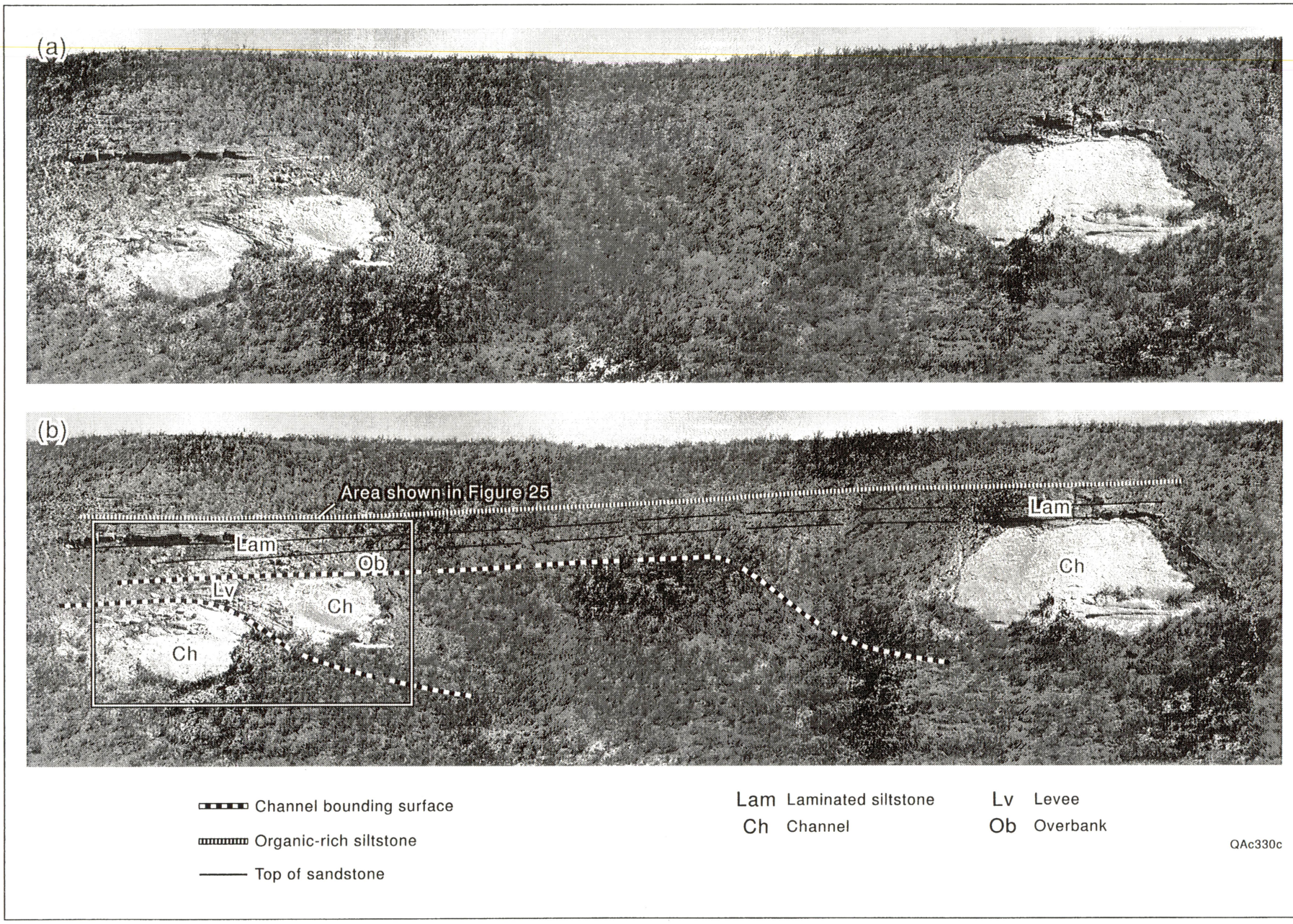

Figure 24. Photograph showing correlation of offset channels within high-order cycle. Photograph is from Willow Mountain between lithologic logs 8 and 10A.

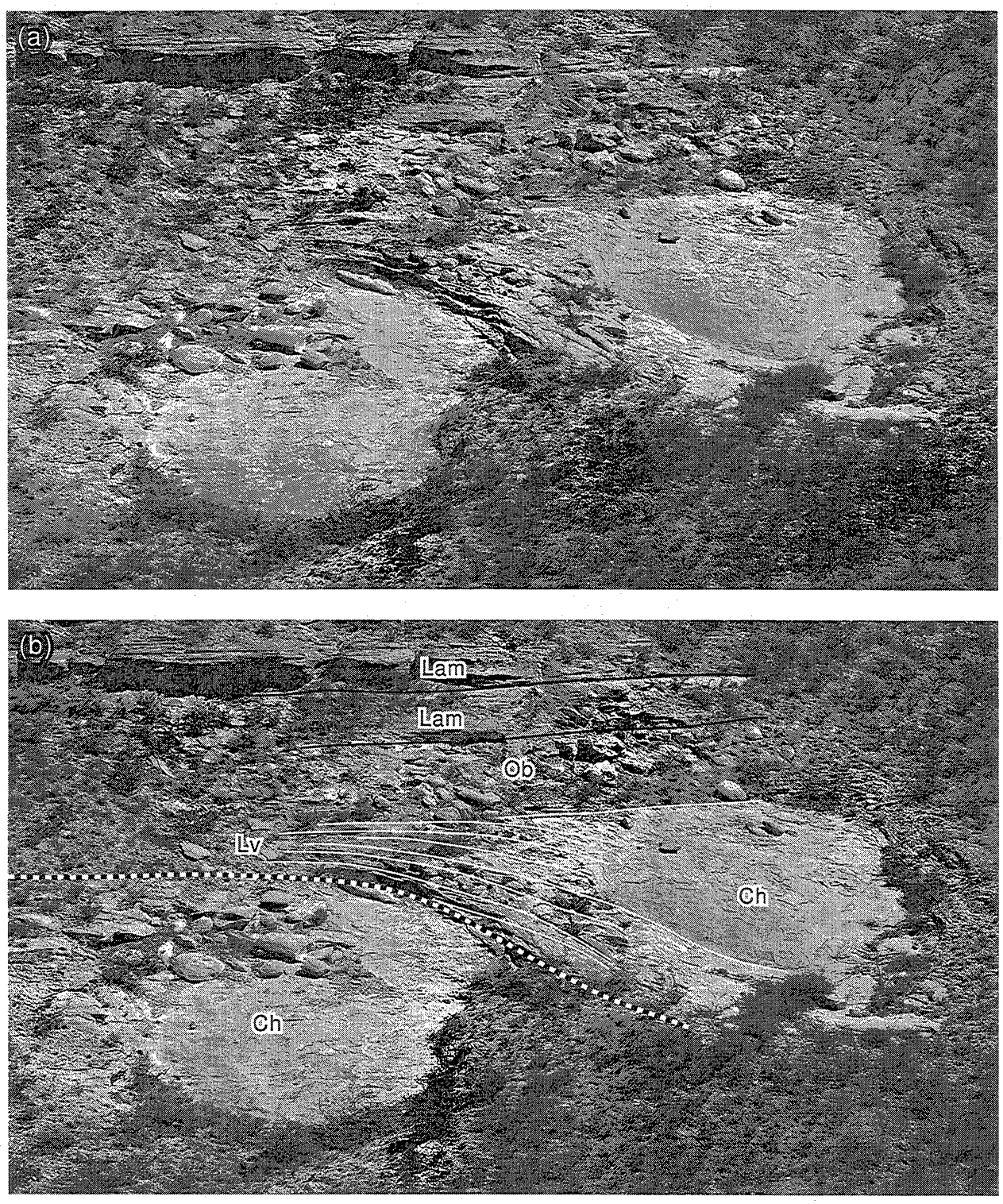

Figure 25. Photograph of channel-levee deposit seen in Figure 24.

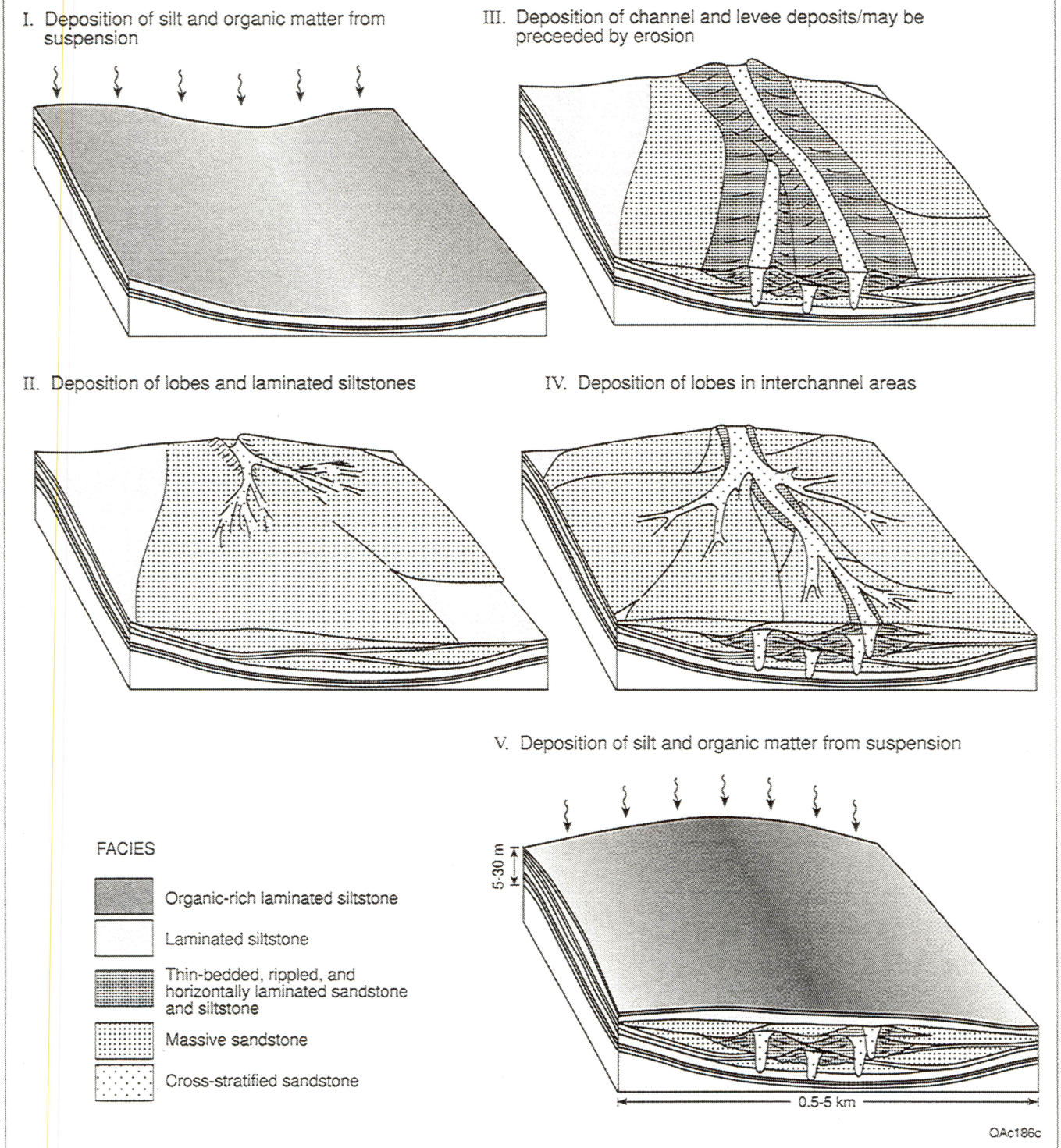

Figure 26. Diagram illustrating depositional facies model for high-order cycle examined at Willow Mountain.

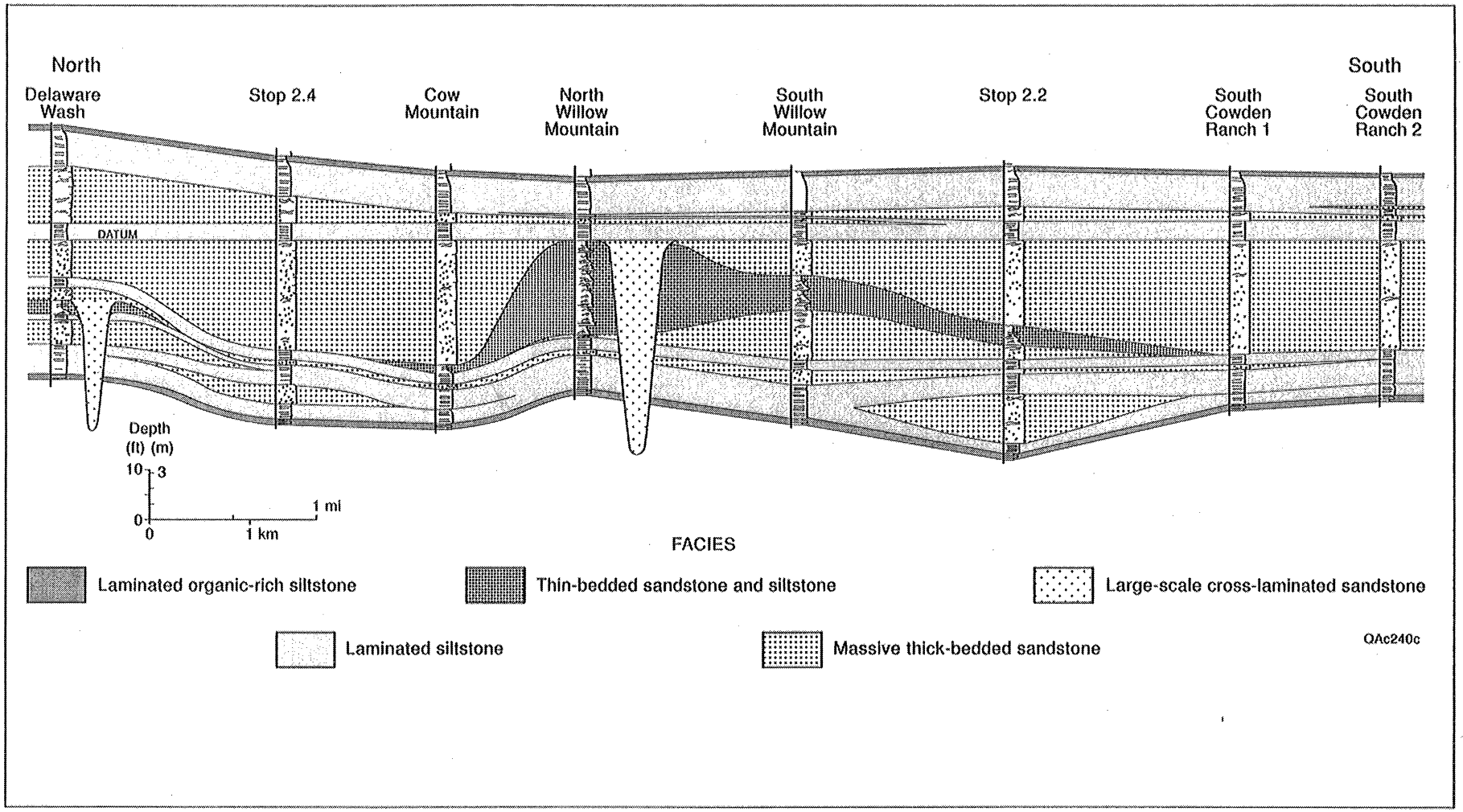

Figure 27. Cross section showing distribution of facies and traces of key surfaces within single high-order cycle. Cross section extends south from Delaware Wash for a distance of about 7 mi.

relate with channel-levee and lobe complexes that are older and younger, respectively, than the one exposed at Willow Mountain. Individual channel-levee and lobe complexes appear to be several tens of kilometers in width. However, the lack of outcrop exposure does not allow the limits of these elements to be defined with much precision. The complexes appear to stack in an offset pattern. Thickening and thinning of sandstones between complexes suggests their arrangement is related to topography, with succeeding systems avulsing into topographic lows.

A final observation worth noting is the fact that the thickness of the laminated siltstones within the high-order cycle remains relatively constant from one end of the cross section to the other. Changes in thickness within the high-order cycle are largely related to increases or decreases in sandstone thickness. The constant thickness of the laminated siltstones also suggests they would be useful correlation markers at the reservoir and field scale.

Acknowledgments

Financial support for this research and field trip were provided by the U.S. Department of Energy under contract no. DE-FC22-95BC14936 (Shirley Dutton, Principal Investigator), by Conoco, Inc., by the Petroleum Technology Transfer Council (PTTC), Texas Region, and by the State of Texas under State Match Pool Project 4201 and the State of Texas Advanced Resource Recovery Project (STARR) (Roger Tyler, Principal Investigator). Final figures were drafted by Kerza A. Perwitt, William C. Bergquist, David M. Stephens, Christian Conly, Jana S. Robinson, and Patrice A. Porter under the direction of Joel L. Lardon. Text was edited by Nina Redmond under the direction of Susann Doenges. Typesetting and layout of the manuscript were completed by Susan Lloyd. Cover design was done by Jamie H. Coggin. Shirley Dutton handled the organization and logistics of the field trip. I would like to thank George Asquith, Andy Cole, Shirley Dutton, Scott Hamlin, Mohammad Malik, Ken Pittaway, and Roger Tyler for their assistance during the field trip. In particular, I would like to thank Tom Cowden, of the Cowden Ranch, for permission to conduct fieldwork on the ranch.

References

Allen, J. R. L., 1982, Studies in fluviatile sedimentation: Bars, bar-complexes, and sandstone sheets (low-sinuosity braided streams) in the Brownstones (L. Devonian), Welsh Borders: Sedimentary Geology, v. 33, 237–293.

Barton, M. D., 1997, Basin floor fan and channel-levee complexes, Permian Bell Canyon Formation: Dallas, Texas, 1997 American Association of Petroleum Geologists Annual Convention, Official Program, v. 6, p. A9.

Berg, R. R., 1979, Reservoir sandstones of the Delaware Mountain Group, southeast New Mexico, *in* Sullivan, N. M., ed., Guadalupian Delaware Mountain Group of West Texas and southeast New Mexico, Symposium and Field Trip Conference Guidebook: Society of Economic Paleontologists and Mineralogists (Permian Basin Section) Publication 79-18, p. 75–95.

Bouma, A. H., 1962, Sedimentology of some flysch deposits: a graphic approach to facies interpretation: Amsterdam, Elsevier, 168 p.

_____ 1996, Initial comparison between fine- and coarse-grained submarine fans and the Brushy Canyon Formation sandstones: the Brushy Canyon play in outcrop and subsurface: concepts and examples: Guidebook, Permian Basin Section, SEPM, Publication No. 96-38, p. 41–59.

Bozanich, R. G., 1979, The Bell and Cherry Canyon Formations, Eastern Delaware Basin, Texas: lithology, environments, and mechanisms of deposition, *in* Sullivan, N. M., ed., Guadalupian Delaware Mountain Group of West Texas and southeast New Mexico, Symposium and Field Trip Conference Guidebook: Society of Economic Paleontologists and Mineralogists (Permian Basin Section) Publication 79-18, p. 121–141.

Fischer, A. G., and Sarnthein, M., 1988, Airborne silts and dune-derived sands in the Permian of the Delaware Basin: Journal of Sedimentary Petrology, v. 58, p. 637–643.

Friend, P. F., 1983, Towards the field classification of alluvial architecture or sequences, *in* Collinson, J. D., and Lewin, J., eds., Modern and ancient fluvial systems: International Association of Sedimentologists Special Publication, No. 6, p. 345–354.

Gardner, M. H., 1992, Sequence stratigraphy of eolian-derived turbidites: patterns of deep water sedimentation along an arid carbonate platform, Permian (Guadalupian) Delaware Mountain Group, West Texas, *in* Mruk, D. H., and Curran, B. C., eds., Permian Basin exploration and production strategies: applications of sequence stratigraphic and reservoir characterization concepts: West Texas Geological Society Publication 92-91, p. 7–12.

_____ 1997, Characterization of deep-water siliciclastic reservoirs in the upper Bell Canyon and Cherry Canyon Formations of the northern Delaware Basin, Culberson and Reeves Counties, Texas, *in* Major, R. P., ed., Oil and gas on Texas State Lands: an assessment of the resource and characterization of type reservoirs: The University of Texas, Bureau of Economic Geology Report of Investigations No. 241, p. 137–146.

Harms, J. C., 1968, Permian deep-water sedimentation by nonturbid currents, Guadalupe Mountains, Texas: Geological Society of America Special Paper 121, 127 p.

_____ 1974, Brushy Canyon Formation, Texas: a deep-water density current deposit: Geological Society of America Bulletin, v. 85, p. 1763–1784.

Harms, J. C., and Williamson, C. R., 1988, Deep-water density current deposits of Delaware Mountain Group (Permian), Delaware Basin, Texas and New Mexico: American Association of Petroleum Geologists Bulletin, v. 72, p. 299–317.

Hiss, W. L., 1975, Stratigraphy and groundwater hydrology of the Capitan aquifer, southeastern New Mexico and western Texas: University of Colorado, Ph.D. dissertation, 396 p.

Jacka, A. D., Thomas, C. M., Beck, R. H., Williams, K. W., and Harrison, S. C., 1969, Guadalupian depositional cycles of the Delaware Basin and Northwest Shelf, *in* Cyclic sedimentation in the Permian Basin: West Texas Geological Society, Symposium p. 152–196.

Jacka, A. D., 1979, Deposition and entrapment of hydrocarbons in Bell Canyon and Cherry Canyon deep-sea fans of the Delaware Basin, *in* Sullivan, N. M., ed., Guadalupian Delaware Mountain Group of West Texas and southeast New Mexico, Symposium and Field Trip Conference Guidebook: Society of Economic Paleontologists and Mineralogists (Permian Basin Section) Publication 79-18, p. 104–120.

Kerans, Charles, Fitchen, W. M., Gardner, M. H., Sonnenfeld, M. D., Tinker, S. W., and Wardlaw, B. R., 1992, Styles of sequence development within uppermost Leonardian through Guadalupian strata of the Guadalupe Mountains, Texas and New Mexico, *in* Mruk, D. H., and Curran, B. C., eds., Permian Basin exploration and production strategies: applications of sequence stratigraphic and reservoir characterization concepts: West Texas Geological Society Publication 92-91, p. 1–6.

Kerans, Charles and Fitchen, W. M., 1995, Sequence hierarchy and facies architecture of a carbonate-ramp system: San Andres Formation of the Algerita Escarpment and western Guadalupe Mountains, West Texas and New Mexico: The University of Texas at Austin, Bureau of Economic Geology, Report of Investigations No. 235, 86 p.

Kneller, B., 1996, When is a turbidity current not a turbidity current? A question of mobility? (abs.): American Association of Petroleum Geologists Annual Convention, Official Program, v. 5, p. A76.

Lowe, D. R., 1982, Sediment gravity flows: II. Depositional models with special reference to the deposits of high-density turbidity currents: Journal of Sedimentary Research, v. 52, p. 279–297.

Meissner, F. F., 1972, Cyclic sedimentation in Middle Permian strata of the Permian Basin, West Texas and New Mexico, *in* Cyclic sedimentation in the Permian Basin (2d ed.): West Texas Geological Society, p. 203–232.

Miall, A. D., 1985, Architectural-element analysis: a new method of facies analysis applied to fluvial deposits: Earth Science Reviews, v. 22, p. 261-308.

Mutti, E., and Normark, W. R., 1987, Comparing examples of modern and ancient turbidite systems: problems and concepts, *in* Leggett, J. K., and Zuffa, G. G., eds., Marine clastic sedimentology: concepts and case studies: London, Graham and Trotman, p. 1–38.

Payne, M. W., 1976, Basinal sandstone facies, Delaware Basin, West Texas and southeast New Mexico: American Association of Petroleum Geologists Bulletin, v. 60, p. 517–527.

Ruggiero, R. W., 1985, Depositional history and performance of a Bell Canyon sandstone reservoir, Ford-Geraldine field, west Texas: The University of Texas at Austin, Master's thesis, 242 p.

Sonnenfeld, M. D., 1991, High-frequency cyclicity within shelf-margin and slope strata of the upper San Andres sequence, Last Chance Canyon, *in* Meader-Roberts, Sally, Candelaria, M. P., and Moore, G. E., eds., Sequence stratigraphy, facies and reservoir geometries of the San Andres, Grayburg, and Queens Formations, Guadalupe Mountains, New Mexico and Texas: Permian Basin Section, Society of Economic Paleontologists and Mineralogist Publication 91-32, p. 11–51.

Williamson, C. R., 1977, Deep-sea channels of the Bell Canyon Formation (Guadalupian), Delaware Basin, Texas–New Mexico, *in* Hileman, M. E., and Mazzullo, S. J., eds., Upper Guadalupian facies, Permian reef complex, Guadalupe Mountains New Mexico and West Texas: Society of Economic Paleontologists and Mineralogists (Permian Basin Section) Publication 77-16, p. 409–431.

_____ 1978, Depositional processes, diagenesis and reservoir properties of Permian deep-sea sandstones, Bell Canyon Formation, Texas-New Mexico: The University of Texas at Austin, Ph.D. dissertation, 262 p.

_____ 1979, Deep sea sedimentation and stratigraphic traps, Bell Canyon Formation (Permian), Delaware Basin, *in* Sullivan, N. M., ed., Guadalupian Delaware Mountain Group of West Texas and southeast New Mexico, Symposium and Field Trip Conference Guidebook: Society of Economic Paleontologists and Mineralogists (Permian Basin Section) Publication 79-18, p. 39–74.

Zelt, F. B., and Rossen, C., 1995, Geometry and continuity of deep-water sandstones and siltstones, Brushy Canyon Formation (Permian) Delaware Mountains, Texas, *in* Pickering, K. T., Hiscott, R. N., Kenyon, N. H., Ricci Lucchi, F., and Smith, R. D. A., eds., Atlas of deep water environments, architectural style in turbidite systems: London, Chapman & Hall, p. 167–183.